A Study of Gene Therapy for Human Salivary Gland Tumors; Wild-Type *KGFR/FGFR2-IIIb* Gene Induces Differentiation and Apoptosis in Salivary Gland Adenocarcinoma Cells *In Vitro* and *In Vivo*

Thesis by

Yan Zhang

Department of Molecular Oral Medicine
and Maxillofacial Surgery 1

Hiroshima University Faculty of Dentistry

Japan

Academic Supervisor

Prof. Tetsuji Okamoto, D.D.S., Ph.D.

2000

Acknowledgements

My sincere gratitude first goes to Professor Tetsuji Okamoto, Department of Molecular Oral Medicine & Maxillofacial Surgery 1, Hiroshima University Faculty of Dentistry for his adequate guidance, encouragement, and supervision throughout my Ph. D. course at Hiroshima University.

I also appreciate Professor Yukio Kato, Department of Biochemistry, Hiroshima University Faculty of Dentistry and Professor Toshihiro Dohi, Department of Pharmacology, Hiroshima University Faculty of Dentistry, for their valuable discussions and suggestions on my work. I am also grateful to Dr. Shigeaki Toratani, Dr. Yasutaka Hayashido, Dr. Yoshiharu Tanaka and Dr. Akihiko Sakamoto for their helpful advices and assistances for this study. I also thank Dr. Mikio Kan and Professor W. L. McKeehan, Center for Cancer Biology and Nutrition, Albert Alkek Institute of Biosciences and Technology and Department of Biochemistry and Biophysics, Texas A&M University, USA., for their generous gift of recombinant KGF and comments for my study. And, I obliged to all the staff members in Department of Oral Molecular Medicine & Maxillofacial Surgery 1, Hiroshima University Faculty of Dentistry, for their kindness and support for me. I extend my thanks to all the staff of Research Facilities for Laboratory Animal Science and Radioisotope Experiment Center for their help and assistance on my study.

Finally, I will give my sincere gratitude to my parents and my younger sister for their intimate love.

This work was supported by a Grant-in Aid for Scientific Research for Research Fellow of Japan Society for the Promotion of Science (#05194).

Contents

Abstract

Malignant salivary gland tumors are devastating neoplasms associated with a poor prognosis in the head and neck regions.

It has been reported that malignant salivary gland tumors exhibited enhanced both fibroblast growth factor (FGF)-1 and FGF-2 expression in comparison with normal salivary glands and that FGF-1 and FGF-2 can act in an autocrine manner to stimulate the proliferation of salivary gland adenocarcinoma cells as a result of an exogeneous receptor-dependent pathway.

In addition, it has also been reported that normal salivary gland epithelial cells and benign salivary gland tumors exclusively express KGFR/FGFR2-IIIb which recognizes stromal cell-derived KGF, and that in the process of malignant transformation of salivary gland tumors, the expression of KGFR/FGFR2-IIIb disappeared and an abnormal activation of FGFR1-IIIc gene expression which recognizes tumor-derived FGF-2 was observed. The exclusive expression of the KGFR/FGFR2-IIIb in both normal and premalignant salivary epithelial cells well correlates with slowly growing and differentiated phenotype of premalignant tumors. In contrast, the complete loss of KGFR/FGFR2-IIIb, and the abnormal expression of both FGFR1 and its ligand FGF-2 in malignant tumor cells are well associated with emergence of the malignant phenotype.

From these lines of evidence, I have proposed following hypothesis that KGF-KGFR system works as an important signal to maintain normal growth and differentiation phenotype of salivary gland, and that KGFR/FGFR2-IIIb might inhibit growth and induce differentiation of salivary gland adenocarcinoma cells by recovering normal phenotype which responds to stroma-derived

KGFR/FGFR2-IIIb gene in growth, differentiation and apoptosis of human malignant salivary gland adenocarcinoma cell line HSY *in vitro* and *in vivo*.

HSY was transfected with wild-type *KGFR/FGFR2-IIIb* gene in pcDNA 3.1/zeo mammalian expression vector. After isolating Zeocin-resistant HSY, HSY overexpressing KGFR was cloned and designated HSY$_{R2\text{-}IIIb}$. HSY transfected with pcDNA 3.1/zeo (HSYzeo) was used as a control.

Effects of FGF-1, FGF-2 and FGF-7/KGF on growth, diferentiation and apoptosis of HSYzeo and HSY$_{R2\text{-}IIIb}$ were studied in serum-free culture. In additon, apoptosis-related MAPK (MEK1/2, p38, JNK/SAPK) and caspase-3 (CPP32) activities upon stimulation with FGFs were examined in both cells. Furthermore, growth rate, differentiation capacity and tumorigenicity of HSYzeo tumors and those of HSY$_{R2\text{-}IIIb}$ tumors were evaluated. Finally, direct gene transfer of *KGFR* gene by electroporation was carried out against HSY tumors in athymic nude mice to study the effects KGFR on tumor growth and differentiation *in vivo*. Following results were obtained:

1. The growth of HSY$_{R2\text{-}IIIb}$ in serum-free medium was significantly reduced compare to that of HSYzeo. None of FGFs stimulated growth of HSY$_{R2\text{-}IIIb}$.

2. TUNEL positive cells, DNA ladder formation and the increase of CPP32/Caspase-3 activity were observed in HSY$_{R2\text{-}IIIb}$ upon stimulation with KGF.

3. FGF-1 and FGF-2 stimulated the phosphorylation of both MEK1/2 and p38 MAPK in HSY and HSYzeo. In contrast, FGF-1, FGF-2 and KGF stimulated the phosphorylation of MEK1/2 but not of p38 and JNK/SAPK in HSY$_{R2\text{-}IIIb}$ and SGE.

4. Growth rate of HSY$_{R2\text{-}IIIb}$ tumors in athymic nude mice was dramatically reduced compare to that of HSYzeo. Some of HSY$_{R2\text{-}IIIb}$ clones

dramatically reduced compare to that of HSYzeo. Some of $HSY^{R2\text{-}IIIb}$ clones lost their tumorigenicity. By histological examination, $HSY^{R2\text{-}IIIb}$ tumors exhibited differentiated morphology such as acinar-like and duct-like structure.

5. KGFR gene therapy starting at one week after HSY cell inoculation, completely cured HSY tumors and that starting at 2-4 weeks significantly inhibited the growth although the tumors did not disappear. Forty eight hours after gene therapy, about 70% of tumor cells exhibited KGFR expression in the nucleus and cytoplasm, and at 4 weeks from gene therapy, about 20% of tumor cells still express KGFR protein in the cytoplasm and cell membrane.

I have shown in this study that wild-type KGFR gene inhibits growth and induces differentiation and apoptosis in HSY cells *in vitro* and *in vivo*. These results strongly suggested the possibility that KGFR gene therapy might be a good alternative to cure salivary gland adenocarcinomas.

Chapter 1 Wild-type KGFR/FGFR2-IIIb inhibits the growth and induces differentiation /apoptosis of human salivary gland adenocarcinoma cells *in vitro* and *in vivo*

1. Introduction

Malignant salivary gland tumors are highly aggressive neoplasms that readily invades adjacent tissues and metastasizes to distant organs at early stages of the disease (Kurokawa, R. 1989). Most current therapeutic approaches, including extensive surgery combined with radiation therapy or chemotherapy, therefore remain palliative, and the prognosis is still extremely poor. Thus, the development of a new modality such as gene therapy is desperately required to overcome this malignancy.

The growth of both normal and transformed cells is controlled by numerous growth factors. The binding of growth factors to their specific receptors on the cell surface may stimulate receptor-associated tyrosine kinase, which transmits mitogenic signals, thus leading to cell proliferation (Szebenyi, G. 1999). Furthermore, neoplastic cells are often found to show altered growth factor synthesis. The amplification and overexpression of growth factors have been observed in human transformed cells, and these phenomena are sometimes correlated with the rapid and invasive growth of the tumor cells (Sporn and Roberts, 1985). Additional evidence relating growth factors to tumor progression comes from the observation that many transformed cells express growth factor receptors that are involved in autocrine growth stimulation (Yoshida, 1990).

Recently, amplification and overexpression of FGF-1, FGF-2 and FGF

receptors have been demonstrated in human tumors and are thought to be important in the malignant growth of neoplasm (Mason, I. J. 1994). Indeed, studies using neutralizing antibodies or anti-sense oligonucleotides indicated that FGF-1 and FGF-2 could act in an autocrine manner to stimulate tumor cell proliferation through an extracellular receptor-dependent pathway (Myoken, Y. 1996). In addition, cells transfected with a coding sequence for FGF-1 or FGF-2 exhibited amplified autocrine growth similar to transformed cells. These data suggest that the elevated expression of FGF-1 and FGF-2 may contribute to cellular transformation and continued cell proliferation (Coughlin, S. R. 1988, Lee, P. L. 1989).

The FGF family consists of a group of homologous polypeptide growth factors that have an affinity with heparin and heparin sulfate-like proteoglycans (Szebenyi, G. 1999). The family includes FGF-1 (acidic FGF) (Burgess, W. H. 1990), FGF-2 (basic FGF) (Eriksson, A. E. 1991, Zhang, J. D. 1991), FGF-3 (int-2) (Murakami, A. 1993), FGF-4 (hst/K-FGF) (Lambe, K. 1996), FGF-5 (Hattori, Y. 1996), FGF-6 (Marics, I. 1989), FGF-7/KGF (keratinocyte growth factor) (Finch, P. W. 1989, Ron, D. 1993), FGF-8 (androgen-induced growth factor) (Gemel, J. 1996), FGF-9 (glial activating factor) (Miyamoto, M. 1993) and FGF-10 (Emoto, H. 1997). Until now, at least 20 members in FGF family have been confirmed.

The prototypic members of the FGF family, FGF-1 and FGF-2 share 55% overall amino acids sequence identity, and have a high affinity for heparin. KGF originally purified from conditioned medium of human embryonic lung fibroblasts, exhibits potent mitogenic activity for a variety of epithelial cell types. KGF contains an amino-terminal signal peptide sequence, and is actively secreted from cells that express it (Rubin, J. S. 1989). However, KGF is distinct from other known FGFs in that it is not mitogenic for fibroblasts or endothelial cells (Finch, P. W. 1989). These features of KGF, and its expression by stromal

cells of a variety of epidermal tissues, suggest that KGF may function as a specific paracrine mediator of normal epithelial cell proliferation.

FGFs transduce their signals to cells by binding to specific cell surface tyrosine kinase receptors (Ullrich, A. 1990, Jaye, M. 1992, Heldin, C. H. 1995). Four closely related receptors have been identified. These receptors are designated FGFR1 (flg), FGFR2 (bek), FGFR3 (JTK4) and FGFR4 (JTK2). Several isoforms of FGFR1, FGFR2 and FGFR3 were also identified: FGFR1-IIIc, FGFR2-IIIb (also named KGFR), FGFR2-IIIc, FGFR3-IIIb, and FGFR3-IIIc (Imamura, T. 1988, Battaro, D. P. 1990, Houssaint, E. 1990, Johnson, D. E. 1991, Kan, M. 1991, Miki, T. 1991, Hou. J. Z, 1991,1992, Kobrin, M. S, 1993, Plotnikov, A. N. 1999).

The roles of FGFs and FGFRs in the development of human normal salivary gland and salivary gland-derived neoplasm have been investigated (Okamoto, T. 1996, Myoken, Y. 1994,1995,1996,1997). Myoken et al have shown that malignant salivary gland tumors exhibit enhanced both FGF-1 and FGF-2 expression in comparison with normal salivary glands by immunohistochemical analysis and that FGF-1 and FGF-2 can act in an autocrine manner to stimulate the proliferation of salivary gland adenocarcinoma cells as a result of an exogenous receptor-dependent pathway by employing neutralizing antibodies or antisense oligonucleotides (Myoken, Y. 1994, 1995, 1996, 1997). These results suggest that the elevated expression of FGF-1 and FGF-2 may contribute to cellular transformation and continued cell proliferation of salivary gland adenocarcinoma cells.

Human salivary gland is composed of well defined epithelial and stromal cell components which communicate to maintain normal gland structure, function and differentiation. The epithelial compartment of benign salivary gland tumors usually exhibits some degree of morphological differentiation that

distinguishes it from the stromal compartment. In contrast, malignant tumors are undifferentiated and exhibit no apparent relationship between epithelial and stromal cells.

Normal salivary gland epithelial cells and benign salivary gland tumors exclusively express the FGFR2-IIIb isoform which recognizes stromal cell-derived KGF and possibly additional KGF homologues (Bottaro, D. P. 1990). In the process of malignant transformation of salivary gland tumors, the expression of KGFR/FGFR2-IIIb isoform disappeared and FGFR1-IIIc gene expression was abnormally activated. The exclusive expression of the KGFR/FGFR2-IIIb isotype in normal and pre-malignant epithelial cell correlates with the response to homologous stromal cells, slowly growing, differentiated pre-malignant phenotype. In contrast, the complete loss of KGFR/FGFR2-IIIb, and the abnormal expression of FGFR1 and its ligand FGF-2 in malignant tumor cells are well associated with emergence of the malignant phenotype.

From these lines of evidence, I have proposed following hypothesis that KGFR/FGFR2-IIIb might inhibit growth and induce differentiation of salivary gland adenocarcinoma cells by recovering normal phenotypes that respond to stroma-derived KGF/FGF-7.

Thus, in this study, I have examined potential role of wild-type KGFR/FGFR2-IIIb gene in human malignant salivary gland adenocarcinoma cell line HSY *in vitro* and *in vivo*.

In this chapter, I provide evidence that the over-expression of KGFR/FGFR2-IIIb depresses the tumor growth and induces differentiation/apoptosis of HSY *in vitro* and *in vivo*.

2. Materials and Methods

2.1. Cell culture conditions

Salivary gland adenocarcinoma cell line, HSY was kindly provided from Professor Mitsunobu Sato (The Second Department of Oral & Maxillofacial Surgery, Tokushima University School of Dentistry, Tokushima, Japan). HSY was maintained in RD medium (RPMI1640 medium : Dulbecco's modified Eagle's medium (DMEM); 1:1) supplemented with 5%CS at 37°C in 5%CO_2 as described previously (Myoken, Y. 1996).

Normal salivary gland-derived epithelial (SGE) cells were isolated from submandibular gland and cultured in serum-free RD153 medium (RPMI1640 medium : DMEM : MCDB153; 1:1:2, v/v/v) containing five factors (10μg/ml bovine insulin, 5μg/ml human transferrin, 10μM β -mercaptoethanol, 10μM 2-aminoethannol and 10 nM sodium selenite) and bovine brain extracts (BBE; prepared in my laboratory) in type-I collagen-coated dishes as described previously (Myoken, Y.1995).

2.2. Lipofectin transfection of HSY

pcDNA3.1/zeo mammalian expression vector (Invitrogen) and pcDNA3.1/zeo- KGFR/FGFR2-IIIb carrying full length FGFR2- IIIb cDNA (Fig.1) which was kindly provided by Dr. W. L. McKeehan (Center for Cancer Biology and Nutrition, Albert B. Alkek Institute of Bioscience and Technology and Department of Biochemistry and Biophysics, Texas A & M University, Houston, TX) were used for transfection.

HSY was seeded at the density of $3x10^4$/ ml on 35-mm culture dish

coated with type-I collagen (Cell Matrix type I-A, Nitta Gelatin Co Ltd., Osaka, Japan) and cultured until 60-80% confluency. The cells were preincubated with serum- and antibiotics-free RD (RD(-)) medium for 2h.

Lipofectamine reagent (GIBCO BRL, Gaitherberg, MD, USA) diluted 1:8 in RD(-) medium to a final volume of 100μl was gently mixed with 2μg DNA (pcDNA3.1/zeo vector or pcDNA3.1/zeo-KGFR/FGFR2-IIIb cDNA) diluted in RD (-) medium to a final volume of 100μl, and then incubated for 30min at room temperature. An additional 800μl of RD(-) medium was added to the mixture, which was then gently overlayed onto HSY. The cells were cultured for 2 to 24h at 37°C in a 5%CO_2 incubator, and RD(-) medium containing 10%CS were added. After a further 48h incubation, the cells were treated EDTA-trypsin and subcultured at 1:10 split ratio in RD(-) containing 10%CS and Zeocin (400μg/ml). Several Zeocin-resistant cells were cloned after 2 weeks. The clones transfected with pcDNA3.1/zeo-KGFR/FGFR2-IIIb cDNA were designated $HSY_{R2\text{-}IIIb}$. The clones transfected with pcDNA3.1/zeo vector were designated HSYzeo.

2.3. Iodination of KGF with Na [^{125}I]

Iodination of KGF was carried out at room temperature in an iodination hood. Briefly, recombinant KGF which was kindly provided by M. Kan (Center for Cancer Biology and Nutrition, Albert B. Alkek Institute of Bioscience and Technology and Department of Biochemistry and Biophysics, Texas A & M University, Houston, TX) was radiolabeled with Na [^{125}I] (NEN, Boston, MA) by the modified chloramine-T method (Kan, M. 1991). Briefly, KGF (2.0μg in 100μl of 250 mM PBS), Na [^{125}I] (1mCi/9.85μl) and chloramine-T (400μg/ml) (Katayama Chemical) were mixed and incubated for 90 seconds at room

temperature. Then, the reaction was terminated by adding 10mM dithiothreitol (DTT) (Wako Pure Chemical Industries. Ltd. Osaka, Japan). After a further 10min incubation, the mixture was applied to the heparin-Sepharose CL-6B column (Pharmicia LKB, Biotechnology AB, Upsala, Sweden) preequilibrated with PBS. After washing the column with PBS containing 0.5M NaCl, [^{125}I] -KGF was eluted with 0.65M NaCl.

2.4. Receptor binding assay

HSYzeo and HSY$_{R2\text{-}IIIb}$ were seeded at 3×10^3/well in type-I collagen-coated 48-well culture plate and cultured for 72 h. The cells were washed with RD binding buffer (RD containing 25mM Hepes and 0.1% BSA, pH 7.4), and incubated with [^{125}I]-KGF (specific activity: $2.74 \times U\, 10^5$ cpm/ng) and various concentrations of unlabeled KGF for 3h at room temperature. Then, the cells were washed twice with ice-cold binding buffer and solubilized with 1% Triton-X 100 in phosphate buffer saline. Aliquot radioactivity was counted with autowell γ-counter (Aloka). Cell numbers were determined as the mean number of cells in duplicate experiments. The Scatchard method was used for analysis of the binding data.

2.5. Reverse transcription-polymerase chain reaction (RT-PCR) and PCR-Southern hybridization

Total cellular RNA was extracted by the acid guanidium thiocyanate-phenol-chloroform (AGPC) method. One μg of total RNA was reverse transcribed by Superscript reverse transcriptase and random hexamers. Subsequent amplification was carried out with Gene-Amp Kit (Perkin-Elmer

Cetus Instrument Co. Ltd. USA) and gene-specific primers for 10 to 35 cycles under the following conditions: 95°C for 1 min, 60°C for 1 min, 70°C for 1 min. Primers for amplification were as follows: 5'-AACGGGAAGGAGTTTAAGCAG-3' and 5' -GGAGCTATTTATCCCCGAGTG-3' for the portion cording of the second half of the third immunoglobulin-like loop of KGFR/FGFR2-IIIb, generating a 328-bp fragment; 5'-CTAGGTTCGTATTTATGTGG-3' and 5'-ACCTGAGTAGCATCATTATAG-3' for α -amylase, generating a 230-bp fragment. The amplification products were electrophoresed on a 1.2% agarose gel and then visualized by ethidium bromide staining.

PCR amplification products of KGFR/FGFR2-IIIb were also electrophoresed on a 1.2% agarose gel and transferred to Biodyne-N membrane (Pall Biosupport Division, East Hills, NY) by capillary blotting and cross-linked by UV treatment. The cDNA probe for KGFR/FGFR2-IIIb which was labelled with [^{32}P] -dCTP (3000Ci/mmol; Amersham, Arlington Height, IL) by ramdom priming method. The membrane was prehybridized in hybridization buffer (6 x SSC, 0.5 x Denhardt's solution, 0.5% SDS, 500 mM EDTA and 100μg/ml salmon sperm DNA) for 3 h at 68°C and hybridized in hybridization buffer containing [^{32}P] -labelled cDNA probe overnight at 68°C. After hybridization, the membrane was washed with 2 x SSC containing 0.1% SDS and 0.2 x SSC containing 0.1%SDS. Then, the membrane was dried and exposed to XAR-5 film (Kodak, Rochester, NY) at -80°C.

2.6. Northern hybridization

Total cellular RNA (20μg) of HSYzeo and HSY$_{R2\text{-}IIIb}$ denatured by glyoxalation, was electrophoresed on 1% agarose-formaldehyde gels, and transferred to Biodyne-N membrane. The membrane was hybridized to

[^{32}P] -labeled cDNA probe in formamide hybridization solution overnight at 68°C, and then exposed to XAR-5 X-Omat film as described for PCR-Southern hybridization.

2.7. Immunocytochemical and immunofluorecent staining

HSYzeo and HSY$_{R2\text{-}IIIb}$ were cultured on Lab-Tek II chamber slide (Nalgen Nunc International, USA) for two days. The cells were fixed with 2% paraformaldehyde (PFA) in PBS for 30min and washed 3 times with PBS. After blocking with 10% normal goat serum for 30min, the cells were incubated with rabbit anti-human amylase antibody (DAKO, A/S, Denmark) diluted 1:100 or rabbit anti-human lactoferrin antibody (DAKO, A/S, Denmark) diluted 1:100. Immunodetection of the antigens was performed using *Elite* avidin-biotin-immunoperoxidase system (Vector Laboratories, Burlingame, CA, USA) according to the manufacture's instruction.

To detect CPP32, the cells were incubated with mouse CPP32 (inactive form) antibody (DAKO, A/S, Denmark, kindly supplied from Dr. Takada, Department of Oral Pathology, Hiroshima University Faculty of Dentistry, Hiroshima, Japan) which recognize inactive form of CPP32 diluted 1:100 in PBS with 0.1%BSA for 1h at 37°C, followed by the incubation with fluorescein-conjugated goat anti-mouse IgG antibody (DAKO, A/S, Denmark) diluted 1:40 in PBS with 0.1%BSA for 1 h at 4°C. After washing with PBS, they were mounted with buffered glycerol, and then viewed with a Nikon fluorescence microscopy (Nikon) .

2.8. Cell proliferation assay

HSYzeo and HSY$_{R2\text{-}IIIb}$ ($3x10^3$/well) were seeded in type I collagen-coated 24-well culture plate, and cultured in serum-free RD5F medium in the presence of indicated concentrations of FGF-1, FGF-2 or KGF for 6 days. The number of cells was measured at indicated periods with Coulter Counter (Coulter Electronics Inc. Hialeah, FL) .

2.9. Trypan blue dye exclusion assay

HSYzeo and HSY$_{R2\text{-}IIIb}$ cultured in serum-free RD5F, were suspended in RD medium containing 5%CS and mixed with equal volume of 0.5% Trypan blue (Wako Chemical) solution. The number of stained cells was counted under light microscope.

2.10. Detection for apoptotic DNA fragmentation

HSY, HSYzeo and HSY$_{R2\text{-}IIIb}$ cultured in serum-free RD5F, were lysed and incubated with 10mM Tris-HCl (pH.8.0) containing 10mM EDTA, 10 mM NaCl, 500μg/ml proteinase K (Sigma. Chemical. Co.), 500μg/ml RNase (Sigma Chemical Co. Tokyo, Japan) and 1%SDS for 3 h at 37°C. Followed by incubation with 26mM Tris-HCl (pH.8.0) containing 6M NaI, 13mM EDTA, 0.5% sodium-N-lauroylsarcosinate and 10mg/ml glycogen for 15min at 60°C. DNA samples precipitated with isopropanol were electrophoresed on a 2% agarose gel and then visualized by ethidium bromide staining to detect DNA fragmentation.

2.11. Terminal deoxynucleotidyl transferase (TdT) mediated dUTP-biotin nick end labeling (TUNEL) assay

Apoptosis of tumor tissues or cultured cells was examined by TUNEL assay using Apoptosis in situ detection Kit. (Wako). HSYzeo and HSY$_{R2\text{-}IIIb}$ were rinsed with PBS, harvested and fixed in 4% PFA for 5 min at room temperature. Then the cells were suspended in PBS and dropped onto the PLL-coated slides (Matsunami Glass Ind. Ltd., Japan). Briefly, the cells were treated with 0.1% trisodium citrate dihydrate solution containing 0.1% Triton X-100 on ice for 2min, and then incubated with TdT reaction solution (TdT enzemy: TdT substrate solution 1:99) for 60min at 37°C. After treated with 3% H_2O_2 for 5min at room temperature and rinsed with PBS, peroxidase-conjugated antibody was added and incubated for 60min at 37°C. The reaction was developed with diaminobenzidine (DAB)-H_2O_2 substrate.

Paraffin sections (4-6μm) of tumor specimen were adhered to PLL-coated slides. After routine deparaffinization and rehydration, tissue sections were digested with proteinase K (20μg/ml in PBS) for 5min at 37°C. The antibody reactions and visualization were performed in the same manner mentioned above.

2.12. CPP32/Caspase-3 activity assay

CPP32/Caspase-3 activity was examined by fluorometric assay with CPP32/Caspase-3 Fluorometric Protease Assay Kit (Medical & Biological Laboratories Co., Ltd. Japan). Briefly, HSYzeo and HSY$_{R2\text{-}IIIb}$ were cultured for 48h in the presence or absence of KGF (20ng/ml), then the cells ($1x10^6$) were resuspend in 50 μl of ice-cold Cell Lysis Buffer for 10min. After reacted with 50μl of Reaction Buffer containing 10mM DTT, cell lysates were incubated with 5μl of the 1 mM DEVD-AFC substrated at 37°C for 2h. The CPP32 activity was

obtained to measure the strength of fluorescence at 505nm activated at 400nm with Spectrophotometer (850 HITACHI Co. Japan).

2.13. Inoculation of the tumor cells in athymic nude mice

Four-week old athymic nude mice (balb/c, AnNCrj-nu/r) were maintained at 24.5°C with 65% relative humidity and fed standard laboratory diet and water.

HSY, HSYzeo and HSY$_{R2\text{-}IIIb}$ (2 x 10^6) suspended in 100μl of PBS were injected to athymic nude mice subcutaneously in the lateral back region. Growing tumor volume (V) were measured twice a week by equation of V=1/2 x length x width ^{2}. Mice were sacrificed by cervical dislocation at 4 weeks after the tumor inoculation. The specimens were fixed in 10% formalin for histological examination, and in 4% PFA for TUNEL assay.

3. Results

3.1. Specific binding of [^{125}I]-KGF to KGF receptors expressed in HSY$_{R2\text{-}IIIb}$

Among Zeocin-resistant HSY, 7 clones exhibiting high binding capacity to KGF were isolated and designated HSY$_{R2\text{-}IIIb}$ (clone 2-4-2, 6-4-3, 6-3-9, 6-1-9, 6-4-5, 24-3-9, 24-2-2). The results of scatchard plots analysis for [^{125}I]-KGF binding to HSY$_{R2\text{-}IIIb}$ clones indicated the presence of a sigle high-affinity receptor population of 0.79-5.66x10^5 sites per cell with an apparent dissociation constant (kd) of 1.48-10.6x10^{-11}M (Table 1).

3.2. Expression of KGFR/FGFR2-IIIb mRNA in the HSY$_{R2\text{-}IIIb}$

Expression of FGFR2-IIIb mRNA in HSY$_{R2\text{-}IIIb}$ was determined by PCR-Southern hybridization and Northern hybridization with [^{32}P]-labeled FGFR2-IIIb cDNA probe. FGFR2-IIIb was expressed in the HSY$_{R2\text{-}IIIb}$ but not in HSY and HSYzeo (Fig.2).

3.3. Phase-contrast morphology of HSYzeo and HSY$_{R2\text{-}IIIb}$

HSY$_{R2\text{-}IIIb}$ exhibited a cobble stone-like appearance with strong intercellular interactions. HSYzeo exhibited a polygonal appearance but more rounded with less intercellular interactions (Fig.3).

3.4. Effects of FGFs on the growth of HSY, HSYzeo and HSY$_{R2\text{-}IIIb}$ in serum-free culture

Both HSY and HSYzeo proliferate well in serum-free RD5F at the doubling time of 16-18 hours whereas HSY$_{R2\text{-}IIIb}$ proliferate very slowly at the doubling time of 52-68 h (Fig.4).

FGF-1 and FGF-2 at 20ng/ml showed a 5 fold stimulation of HSYzeo growth in serum-free culture. None of FGFs stimulated the growth of HSY$_{R2\text{-}IIIb}$ (Fig.5).

3.5. KGFR/FGFR2-IIIb induces cellular differentiation in HSY$_{R2\text{-}IIIb}$

Immunohistochemical study revealed that about 10% of total HSYzeo exhibited weakly positive staining for both α-amylase and lactoferrin, and that about 60% of total HSY$_{R2\text{-}IIIb}$ showed strong positive staining for both in the cytoplasm and perinuclear regions (Fig.6). In addition, semi-quantitative RT-

PCR analysis revealed that α-amylase mRNA was highly expressed in HSY$_{R2\text{-}IIIb}$ and SGE compared to HSYzeo (Fig.7).

3.6. KGFR/FGFR2-IIIb induces apoptosis in HSY$_{R2\text{-}IIIb}$

The viability of HSYzeo and HSY$_{R2\text{-}IIIb}$ cultured in serum-free RD5F containing KGF (20ng/ml) was examined by Trypan blue dye exlcusion assay. As a result, 10% of HSY$_{R2\text{-}IIIb}$ has died on day 2, 15% on day 3, 50% on day 4, and 90% on day 6, although, 10% of HSYzeo has died on day 6 (Fig.8).

Apoptosis of the cells was examined by TUNEL method. TUNEL positive cells were observed in HSY$_{R2\text{-}IIIb}$ although no TUNEL positive cells were detected in HSYzeo (Fig.9A-C). Three days culture of HSY$_{R2\text{-}IIIb}$ with KGF increased the cells with TUNEL positive nuclei to 15%, and the percentage of the cells with positive nuclei increased until 6 days of culture. By increasing culture period of HSY$_{R2\text{-}IIIb}$ with KGF, the intensity of TUNEL staining has also increased in addition to the number of stained nuclei. Furthermore, the cells cultured with KGF exhibited positive nuclei in crescent shape pattern at initial culture period and this staining pattern became more condensed and fragmented in whole nuclei.

No detectable DNA fragmentation was observed in HSY and HSYzeo cultured with KGF (20ng/ml) for 7 days. On the other hand, a typical DNA ladder was observed in HSY$_{R2\text{-}IIIb}$ cultured with KGF (20ng/ml) for 4 days, and was markedly increased over a 7 day-period (Fig.9D).

As Caspase-3/CPP32 protease plays an important role in apoptosis, the activity of Caspase-3/CPP32 in HSYzeo and HSY$_{R2\text{-}IIIb}$ was examined by immunofluorescent and fluorometric assays. Immunofluorescent analysis revealed that the inactive form of caspase-3 was highly expressed in HSYzeo, but not in HSY$_{R2\text{-}IIIb}$ (Fig.10A and B).

Furthermore, fluorometric assay confirmed that the caspase-3 activity in HSY$_{R2\text{-}IIIb}$ cultured with KGF was 16-folds higher than that in HSYzeo. In addition, the activity in HSY$_{R2\text{-}IIIb}$ cultured without KGF was still 8-folds higher than that in HSYzeo. These results suggested that KGFR signal might induce caspase-3 which is responsible for induction of apoptosis (Fig.10C).

3.7. *Growth, differentiation and apoptosis of HSY$_{R2\text{-}IIIb}$ in vivo*

3.7.1. KGFR/FGFR2-IIIb expression reduces tumorigenicity *in vivo*

KGFR/FGFR2-IIIb was able to inhibit growth of HSY cells *in vitro*, thus, I have studied whether KGFR/FGFR2-IIIb expression can suppress the *in vivo* tumorigenicity of the HSY. HSY, HSYzeo and HSY$_{R2\text{-}IIIb}$ clones were inoculated subcutaneously in the lateral back region of athymic nude mice and tumor incidence and growth were monitored.

There was no significant difference between the tumor growth of HSYzeo and parental HSY. In contrast, there was a significant reduction in growth rate of HSY$_{R2\text{-}IIIb}$-derived tumors as compared with that of HSY- and HSYzeo-derived tumors. In addition, 24-3-9, 6-3-9, and 24-2-2 HSY$_{R2\text{-}IIIb}$ clones lost their tumorigenicities (Fig.11).

Thus, it is evident that KGFR/FGFR2-IIIb expression reduced both tumor incidence and tumor growth rate.

3.7.2. Macroscopic appearance of the tumors in athymic mice

HSY-, HSYzeo- and HSY$_{R2\text{-}IIIb}$-derived tumors in athymic nude mice were excised and examined macroscopically. HSY- and HSYzeo-derived tumors exhibited irregularly rounded appearance with lobulated or multinodular surface. The connective tissue which is abundant in

vasucularization did not completely encapsulate the tumors. In contrast, the HSY$_{R2\text{-}IIIb}$-derived tumors were much smaller in size, softer and pale in comparison with HSYzeo tumors and exhibited rounded structures with smooth surface, and well encapsulated and demarcated from the surrounding connective tissues (Fig.12).

3.7.3. Microscopic histological examination of the tumors

The histological appearances of HSY- and HSYzeo-derived tumors exhibited typical adenocarcinomas with solid and trabecular pattern. The tumors were composed of cuboidal cells with occasional isocytism and mitosis. In addition, larger cells which had pale-staining eosinophilic cytoplasm were observed in some areas of the tumors. Although the tumors were surrounded by the pseudocapsule, some groups of neoplastic cells frequently invaded or infiltrated in surrounding fibrous and muscular tissues (Fig.13A).

On the other hand, tumors developed from HSY$_{R2\text{-}IIIb}$ exhibited predominant duct-like and acinar-like stuctures surrounded by stromal cells indicating differentiation was induced (Fig.13B). Upon TUNEL examination, endogenous DNA fragmentation and apoptotic bodies were observed in the nuclei indicating apoptosis (Fig.14).

4. Discussion

Cell growth, differentiation, migration and apoptosis are in part regulated by several polypeptide growth factors and cytokines. Many types of neoplasm exhibit cytogenetic changes that ultimately affect the synthesis of growth-regulating proteins. Switching in expression of FGFR genes has been implicated in the malignant progression of salivary gland tumors from a non-malignant, stromal-dependent epithelial tumor, to an invasive, stromal-independent, undifferentiated tumor such as adenocarcinomas. FGFR2-IIIb expression is abundant in normal salivary gland tissue, benign salivary gland tumors and all low-grade salivary gland tumors, but absent in malignant salivary gland tumors. Conversely, FGFR1-IIIc expression is absent or barely detectable in normal salivary gland but is significantly elevated in malignant salivary gland tumors. Accompanying the switch from exclusive expression of FGFR2-IIIb to FGFR1-IIIc, the reduction in expression of FGFR2-IIIb and the activation of FGFR1 in epithelial cells is the loss of both ductal differentiation and responsiveness to stromal cell-derived KGF.

The growth assay in serum-free culture showed that growth of HSY and HSYzeo were significantly stimulated by FGF-1 and FGF-2, but not by KGF. However, none of them stimulated the growth of $HSY^{R2\text{-}IIIb}$. This result suggests that restoration of the FGFR2-IIIb kinase in human salivary adenocarcinoma cells inhibited growth signals of FGF-1, FGF-2 and KGF.

KGF has potent mitogenic activity for a wide variety of epithelial cells but lacks detectable activity on fibroblasts or endothelial cells. Its synthesis by stromal fibroblasts in a large number of epidermal tissues has suggested that KGF is an important site-directed paracrine mediator for normal epithelial cell proliferation. The salivary gland adenocarcinoma cells HSY is independent on

the KGF secreted by stromal cells, and growth stimulated by FGF-1 and FGF-2 which were produced by itself in an autocrine manner. This autocrine signaling pathway ensures uncontrolled proliferation of malignant cells. The present study indicates that KGFR/FGFR2-IIIb introduced into HSY may alter the autocrine signaling pathway of FGF-2 through FGFR1 and the coupling to other receptor transduction cascades.

The salivary gland is composed of well-defined epithelial and stromal cell components which communicate to maintain normal gland structure and function. The epithelial compartment of benign salivary tumors usually exhibits some degree of morphological differentiation that distinguishes it from the stromal compartment. In contrast, malignant tumors are undifferentiated and exhibit no apparent relationship between epithelial and stromal cells.

In present study, HSY- or HSYzeo-derived tumors in athymic mice exhibited irregularity with lobulated or multinodular at surface, macroscopically. The histopathological structure was similar to undifferentiated adenocarcinomas. In contrast, HSY$_{R2\text{-}IIIb}$-derived tumors exhibited reduced growth rate and some changes in cellular organization and cell-to-cell interactions. The appearance of predominent duct-like and acinar-like structures suggested that the communication between stromal cells and epithelial cells was, to some extent, restored and that cellular differentiation was induced. Thus, it is supeculated that the growth of HSY$_{R2\text{-}IIIb}$-derived tumors was regulated by KGF signal which is recovered by KGFR/FGFR2-IIIb.

An important aspect of cytodifferentiation of normal and neoplastic salivary tissue is the expression of different intermediate filaments, enzymes, immunologic components, and other proteins. In normal salivary gland, acinar cells are immunohistochemically positive to functional markers such as amylase, lactoferrin, lysozyme, secretary component, and structural markers

such as low and high molecular weight keratins and carcinoembryonic antigen (Reitamo, S. 1980). Previous experiments indicated that malignant salivary gland tumor HSG cells are strongly positive to keratin, vimentin, desmin, tropomyosin and carcinoembryonic antigen, weakly positive to lactoferrin and secretory component, and negative to S-100 protein. Immunohistochemical characteristics of the primary and metastatic tumors, which were produced by inoculation of HSG cells into athymic mice indicated that lactoferrin and secretory component were negative in the primary and metastatic tumors (Sato, M. 1985). In present study, 10% of HSY and HSYzeo were both weakly positive in the expression of α-amylase and lactoferrin, and 60% of HSY$^{R2\text{-}IIIb}$ were strongly positive to amylase and lactoferrin by immunohistochemical examination. In addition, semi-quantitative RT-PCR analysis indicated that the expression level of α-amylase mRNA in HSY$^{R2\text{-}IIIb}$ was much higher than that of HSYzeo.

TUNEL positive cells, DNA ladder formation and increase of CPP32/Caspase-3 activity were observed in HSY$^{R2\text{-}IIIb}$ cultured in RD5F and those were further stimulated by KGF. DNA from HSY$^{R2\text{-}IIIb}$ underwent progressive degradation yielding a ladder of DNA fragments corresponding to multimers of nucleosomal-sized DNA. This pattern of degradation indicates typical apoptosis. It was striking that after 4 days culture of HSY$^{R2\text{-}IIIb}$ with KGF, DNA degradation was already evident in the attached and detached cells. Morphological examination revealed that HSY$^{R2\text{-}IIIb}$ demonstrated typical features of cells undergoing apoptosis such as condensation of nucleus and translucent cytoplasmic vacuoles..

In addition, high caspase-3 activity was observed in HSY$^{R2\text{-}IIIb}$ upon stimulation with or without KGF, indicating that HSY$^{R2\text{-}IIIb}$ were undergoing to apoptosis. These results indicated that KGFR/FGFR2-IIIb induced apoptosis in

adenocarcinoma cells *in vitro*.

Apoptosis is induced by a variety of stimuli, such as tumor necrosis factor (Laster, S.M. 1988), Fas ligand, genotoxic compounds (Barry, M.A., et al., 1990), and various environmental stresses (Gavrieli, Y. 1992, Graeber, T. G. 1996, Shian, S. G. 1999). Despite the diversity of apoptosis-inducing agents, numerous experiments indicate that signals leading to the activation of a family of intracellular cysteine proteases, the caspases, may play a pivotal role in the initiation and execution of apoptosis induced by various stimuli. To date, at least 10 different members of caspases in mammalian cells have been identified (Terada, K. 1997, Thornberry, N. A. 1997, He, J. 1998). Among them, the best-characterized caspase is caspase-3, previously called CPP32/Yama/Apopain, which shares an even closer homology with caspase-1. Similar to caspase-1, caspase-3 is synthesized as an inactive proenzyme that requires proteolytic activation. Unlike caspase-1, caspase-3 does not appear to undergo autocatalytic cleavage. This suggests that activation of caspase-3 may involve in another aspartate-specific protease. Once activated, caspase-3 may cleave a variety of substrates, including PARP(poly-ADP-ribose polymerase), DNA-dependent protein kinase, Mr 70,000 subunit of the U1 small ribonucleoprotein, GDP dissociation inhibitor for the Ras-related Rho family GTPases, protein kinase C, and DNA fragmentation factor.

Apoptosis can be found in virtually all untreated malignant tumors, for example, tumor necrosis factor has been shown to induce apoptosis in tumor cell lines in vitro (Lu, C. 1997). In addition, it has been reported that some of the apoptosis observed in tumors *in vivo* may be attributable to release of this cytokine by infiltrating macrophage (Kerr, J. F. 1994).

In $HSY_{R2\text{-}IIIb}$-derived tumor, the apoptotic cell numbers have dramatically increased compared to those in HSYzeo-derived tumors.

Moreover, the apoptotic cells were always localized by stromal cells, indicated that KGF secreted by stromal cells was involved in the induction of apoptosis in $HSY_{R2\text{-}IIIb}$.

These findings strongly support the hypothesis that FGFR2-IIIb plays an important role to maintain normal growth and differentiation phenotype of salivary gland, and that KGFR/FGFR2-IIIb might inhibit growth and induce differentiation of salivary gland adenocarcinoma cells by recovering normal phenotypes which respond to stroma-derived KGF/FGF-7.

Chapter 2 The role of MAPKs in growth, differentiation and apoptosis of salivary gland adenocarcinoma cells

1. Introduction

I have demonstrated in chapter 1 that the overexpression of KGFR/FGFR2-IIIb resulted in differentiation and apoptosis in salivary gland adenocarcinoma cells. There is much interest in how KGFR/FGFR2-IIIb in salivary gland adenocarcinoma cells alter the cancer progression.

FGF receptor binding activates multiple intracellular pathways, the appropriate intergration of these pathways in proliferation, differentiation and apoptosis are crucial for the development, angiogenesis and cancer. The final outcome of FGFR signaling is the result of complicated interplay between activated pathways and feedback loops, and it is also dependent on the amplitude and duration of the signals.

MAPK pathways are cellular signaling pathways that enable cells to transduce extracellular signals into an intracellular response (Robinson, M.J. 1997). In mammalian cells, three parallel MAPK pathways have been identified. The ERK pathway is activated in response to signals from cell surface receptors and has been shown to regulate both cell proliferation and differentiation, depending on the cell context (Marshall, 1995). In contrast, p38 and JNK pathways are primarily activated by cellular stress signals such as inflammatory cytokines, heat shock or UV light and have therefore also been described as stress-activated protein kinases. However, activation of p38 and JNK pathways is not limited to a cellular stress response, since they can also be potently activated by hemopoietic cytokines (Rausch, 1997, Terada, K.

1997, Foltz, I. N. 1997, Crawley, J. B. 1997).

Multiple JNK isoforms have been identified that originate from alternative splicing of three-mammalian gene (Derijard, B. 1994, Kyriakis, J. M. 1994). Similarly, several isoforms of p38 have been described: p38 α, also named CSBP2 or stress-activated protein kinase 2a (Han, J, 1994) p38 β, also named stress-activated protein kinase 2b (Jiang, Y. 1996), and its splice isoform β2; p38 γ, also termed stress-activated protein kinase 3 or ERK6 (Lechner, C. 1996; Cuenda, A. 1997) and p38 σ, otherwise known as stress-activated protein kinase 4 (Wang, X. S. 1997). p38 α and p38 β are the most homologous of this class of MAPKs and are both inhibited by the pyridine-imidazoles SB203580 and SB202190, whereas the γ and σ isoforms are insensitive to these compounds (Goedert, M. 1997).

MAPKs are activated by phosphorylation on Thr and Tyr by dual-specificity MAPK kinases (MAPKKs), which are themselves, activated by MAPKK kinases (MAPKKKs). In addition, small GTPases acting upstream of MAPKKKs are critically involved in the regulation of mammalian MAPK pathways. Upon activation, receptor tyrosine kinases undergo rapid autophosphorylation on numerous tyrosine residues. Autophosphorylation sites located within the catalytic domain are crucial for stimulation of kinase activity, while autophosphorylation sites located in other regions are usually involved in the recruitment of cellular target proteins (Lowenstein, E. J. 1992, Batzer, A. G. 1994).

It is well known that the adaptor protein Grb2 links receptor tyrosine kinases with the Ras signaling pathway by binding to the guanine nucleotide-releasing factor Sos through its SH3 domain and to tyrosine-phosphorylated receptors via its SH2 domain (Clark, 1992; Gale, N. W. 1993, Rozakis Adocock, M.1993, Batzer, A. G. 1994). However, Grb2 does not bind directly to FGF

receptors. The additional cellular protein termed FRS2 become tyrosine-phosphorylated and bind to Grb2 in response to FGF stimulation and thus may link FGF receptors with the Ras/MAPK signaling pathway (Kouhara, H. 1997). Activation of ERKs requires activation of Ras and concomitant activation of Raf family kinases such as Raf-1, which in turn phosphorylate and activate the dual specificity kinase MEK, MEK then phosphorylates ERKs on Thr and Tyr, resulting in ERK activation. (Li, N. 1993, Marshall, C. J. 1995). Dual specificity kinases that activate JNK are MKK4/SEK-1 (Derijard, B. 1994) and MKK7, whereas MKK3 and MKK6 have been identified as activators of p38, displaying some degree of selectivity for individual p38 isoforms (Enslen, H. 1998, Raingeaud, J. 1996).

It is clear that Ras is a key mediator of growth factor-dependent cell survival. Of the various pathways that are activated by Ras, the pathway that comprises the series of sequentially activated protein kinases Raf-MEK-ERK has been found to promote cell survival and inhibit apoptosis (Meier, P. 1997, Kurada, P. 1998, Xia, Z. 1998).

As described in Chapter 1, overexpression of *KGFR/FGFR2-IIIb* gene induced apoptosis in HSY. To understanding the differences of the Ras-MAPK signaling pathway in HSYzeo and in HSY$^{R2\text{-}IIIb}$, the mechanisms by which this signaling cascade suppresses the components of cell proliferation machinery were studied in this chapter.

2. Materials and methods

2.1. Antibodies and reagents

Anti-phosphotyrosine mouse monoclonal antibody was purchased from Upstate biotechnology (clone 4G10), anti-Grb2 antibody was from Transduction Laboratories (Lexington KY mouse monoclonal IgG1), and goat anti-FRS2 serum was from Santa Cruz Biotechnology. PhosphoPlus^{TM} SAPK/JNK (Thr183/Tyr185) Antibody Kit, PhosphoPlus^{TM} p38 MAP Kinase (Thr180/Tyr182) Antibody Kit, and PhosphoPlus^{TM} MEK1/2 (Ser217/221) Antibody Kit were purchased from New England Bio Labs. Specific MEK inhibitor PD098059 and specific p38 MAPK inhibitor SB203580 were purchased from CALBIOCHEM.

2.2. Analysis of phosphorylated proteins associated with Grb2

HSYzeo, HSY$_{R2\text{-}IIIb}$ and SGE cells were starved in RD medium or RD153 medium for 24 h, and then incubated with 20 ng/ml of FGF-1, FGF-2 or KGF for 5 min at 37°C. The cells were washed three times with cold PBS containing 1mM Na_3VO_4, and lysed with RIPA buffer (50mM HEPES, 1% Triton X-100, 10% glycerol, 150mM NaCl, 100mM NaF, 1.5mM $MgCl_2$, and 1mM EGTA, 1mM Na_3VO_4, 1mM PMSF and 10μg/ml aprotinin). The lysates were sonicated, and clarified by centrifugation at 12,000xg for 20min. The lysates were incubated with protein A Sepharose CL-4B (Pharmacia Biotech, Uppsala, Sweden) and centrifuged at 12,000xg for 5min. The supernatants were immunoprecipitated with anti-Grb2 antibody and protein A-Sepharose

CL-4B overnight at 4°C. The pelleted beads were washed three times with NET-gel buffer (50mM Tris-HCl, 150mM NaCl, 0.1% Nonidet P-40, 1mM EDTA, 0.25% gelatin, 0.02% Na_3VO_4). The immunoprecipitated samples were electrophoresed on a 10%SDS-polyacryamide gel under reducing condition and transfered to Immobilon-P membrane. The membrane was blocked with 10mM Tris-HCl (pH 7.4) containing 100 mM NaCl, 0.1% Tween 20 and 5% non-fat milk for 60 min at room temperature, and incubated with anti-phosphotyrosine antibody overnight at 4°C. Immunodetection of the antigen were performed using the BCIP/NBT Membrane Phosphatase Substrate System (Kirkegard & Perry Laboratories, Maryland, USA).

2.3. Analysis of phosphorylation of MAPKs upon stimulation with FGFs

HSYzeo, $HSY_{R2\text{-}IIIb}$ and SGE cells stimulated with 20ng/ml of FGF-1, FGF-2 or KGF for 5min at 37°C were lysed with sample buffer. The samples were subjected to 10%SDS-PAGE and transfered to Immobilon-P membrane. The membrane were blocked with 5% non-fat milk in TBS (50mM Tris-HCl, pH7.6, 150mM NaCl) containing 0.1%Tween-20 for 1h at room temperature, then incubated overnight with anti-phosphorylated MEK1/2, anti-phosphorylated p38, or anti-phosphorylated JNK antibody diluted 1:1000 at 4°C. After washing with TBS containing 0.1%Tween-20 three times, the membranes were incubated with biotinylated secondary antibody diluted 1:2000 and HRP-conjugated anti-biotin antibody diluted 1:1000 for 1 h at room temperature. The antigens were visualized by ECL system (Amersham). The same membranes were stripped with 2%(W/V) SDS, 62.5 mM Tris-HCl (pH 7.0) and 100 mM β-mercaptoethanol for 30min at 60°C, and incubated with

anti-MEK1/2, anti-p38, or anti-JNK antibodies, respectively.

Additionally, the cells pretreated with 20μM PD98059 or 2μM SB203580 at 37°C for 60min, were stimulated with FGF-2 and analyzed for p38 MAPK phosphorylation as described above.

2.4. Immunocytochemical analysis

HSYzeo cultured on Lab-Tek II chamber slide for two days, was starved in RD medium for 24 h, and then stimulated with FGF-2 at 37°C for 5min. After washing with PBS containing 1 mM Na_3VO_4 three times, the cells were fixed with 2% PFA for 30 min at 4°C. The cells were treated with blocking buffer (10% normal goat serum in TBS) for 60min followed by incubation with anti-phosphorylated p38 antibody or p38 antibody (diluted 1:1000 in blocking buffer) for 24h at 4°C. Immunodetection of the antigens was performed using *Elite* avidin-biotin-immunoperoxidase system (Vector Laboratories, Burlingame, CA, USA) according to the manufacture's instruction.

3. Results

3.1. The tyrosine phosphorylation of cellular substrates induced by FGFs in HSYzeo and HSY$_{R2\text{-}IIIb}$

To search for tyrosine-phosphorylated proteins that bind to Grb2 in response to FGF-1, FGF-2 or KGF, cell lysates from HSYzeo, HSY$_{R2\text{-}IIIb}$ or SGE were immunoprecipitated with anti-Grb2 antibody, and then immunoblotted with anti-phosphotyrosine antibody (4G10). In HSYzeo, three of Grb2-associated proteins (p46^{shc}, p52^{shc}, p66^{shc}), and FRS2 were identified as tyrosine phosphorylated proteins. However, in HSY$_{R2\text{-}IIIb}$, only p46^{shc} and p52^{shc} were identified as tyrosine phosphorylated proteins (Fig.15).

3.2. Phosphorylation of MAPKs by FGFs in HSYzeo and HSY$_{R2\text{-}IIIb}$

The antibodies that only recognize the phosphorylated form of MAPKs were used to detect activated MEK1/2, p38 MAPK and JNK.

Both MEK1/2 and p38 MAPK were phosphorylated in HSYzeo upon stimulation with either FGF-1 or FGF-2 (Fig.16). On the other hand, MEK1/2 was the only phosphorylated MAPK in both HSY$_{R2\text{-}IIIb}$ and SGE by FGF-1, FGF-2 or KGF stimulation (Fig.17-19). Phosphorylated JNK was not observed in any cells.

3.3. Effects of inhibitors for MAPKs on p38 activity of HSYzeo

Phosphorylation of p38 MAPK in HSYzeo was apparently inhibited by 2μM SB203580 but not by PD98059 indicating that there is no cross-talk between MEK1/2 and p38 MAPK in HSYzeo (Fig.21).

3.4. Immunohistochemical analysis for nuclear translocation of p38 MAPK

The expression and distribution of p38 MAPK in HSYzeo upon stimulation with FGFs were assessed by immunoperoxidase staining with anti-p38 and anti-phosphorylated-p38 antibodies.

In G_0-arrested HSYzeo, positive staining for p38 MAPK was observed in the cytoplasm (Fig.20A), but immuno-negative for phospho-p38 MAPK (Fig.20B). At 5min after stimulation with FGF-1 or FGF-2, both p38 and phosphorylated-p38 were predominantly localized in the nucleus (Fig. 20C and D). At 2 hours after stimulation with FGF-1 or FGF-2, phosphorylated-p38 was uniformly localized in the whole cells (Fig.20E). The addition of p38 MAPK inhibitor SB203580 (5μM) prior to FGF-1 or FGF-2 treatment inhibited nuclear translocation of p38 MAPK in HSYzeo (Fig.20F).

4. Discussion

Unlike EGF and PDGF receptors, FGF receptors do not bind to Grb2 directly upon FGF stimulation. FGF receptors require another lipid-anchored adaptor protein, FRS2 to become tyrosine-phosphorylated and bind to Grb2 in response to FGF stimulation and thus may link FGF receptors with Ras/MAPK signal pathway. FRS2 is phosphorylated on multiple tyrosine residues (Y196, Y306, Y349, Y392, and Y436) that function as docking sites for Grb2-Sos complexes (Kouhara, A. H. 1997, Hadari, Y. R. 1998). In addition, the mammalian Shc gene encodes three overlapping proteins of 46, 52 and 66 KDa ($p46^{Shc}$, $p52^{Shc}$ and $p66^{Shc}$). These polypeptids all contain a carboxy-terminal Src homology 2 (SH2) domain and an adjacent glycine/proline rich region with homology to the collagen α1-chain (CH domain). Shc proteins are phosphorylated on tyrosine by a variety of receptor and cytoplasmic tyrosine kinases. Phosphorylated Shc proteins form a complex with the SH2-SH3 containing Grb2 proteins which is implicated in the regulation of Ras, suggesting that Shc is involved in the intracellular transmission of growth signals from activated tyrosine kinases to Ras.

As FRS2 is a docking molecule for FGFR1 (Hadari, Y. R. 1998), and as Shc are very important for signaling through the Ras pathway, the blockage of FRS2 or Shc phosphorylation would, to some extent, result in the blockage of Ras-MAP kinase phosphorylation.

In this experiment, although similar phosphorylation patterns of Grb2, $p46^{Shc}$ and $p52^{Shc}$ were detected in HSYzeo and $HSY^{R2\text{-}IIIb}$, phosphorylation of FRS2 and $p66^{Shc}$ was undetectable in both $HSY^{R2\text{-}IIIb}$ and SGE. It is considered that HSYzeo and $HSY^{R2\text{-}IIIb}$ express equal amount of FGFR1. If that so, the defect of FRS2 and $p66^{Shc}$ phosphorylation in $HSY^{R2\text{-}IIIb}$ might be

resulted from KGFR/FGFR2-IIIb expression. Thus, it was speculated that KGFR/FGFR2-IIIb signal in HSY$^{R2\text{-}IIIb}$ might dominantly inhibit or regulate FGFR1 signal by interacting with FRS2 or p66^{Shc}.

As the numbers of KGFR in HSY$^{R2\text{-}IIIb}$ is much higher than that of FGFR1, KGFR/FGFR2-IIIb is consider to be dominant in controlling signal transduction in HSY$^{R2\text{-}IIIb}$. The differences in mitogenic potential between FGFR1 and KGFR/FGFR2-IIIb could be due to a difference in the ability of these receptors to become activated after ligand binding. Alternatively, activated FGFRs could have different signaling potentials. It has been reported that overexpression of Shc proteins in cultured fibroblasts induced morphological transformation, continued transit through the cell cycle in the absence of growth factors and malignant transformation (Salcini, A. E. 1994). These data are fully consistent with the proposition that Shc overexpression exerts its transforming activity by forming a constitutive complex with Grb2, and thereby delivering a continuous mitogenic stimulus through the Ras pathway.

In addition, the phosphorylation of p66^{Shc} was detected in HSYzeo but not in HSY$^{R2\text{-}IIIb}$, while the phosphorylation of both p46^{Shc} and p52^{Shc} were observed in both cells. This result suggested the possibilities that the expression of Shc protein was also inhibited by overexpressing KGFR/FGFR2-IIIb in HSY$^{R2\text{-}IIIb}$.

p38 MAPK is the mammalian homologue of yeast HOG kinase and participates in a cascade controlling cellular responses to cytokines and various of stresses. Both MKK3 and SEK phosphorylate p38 on tyrosine and threonine at the sequence T-G-Y resulting in p38 activation. MEK1/2 also called MAP or ERK kinases, are dual specificity protein kinases that function in a mitogen activated protein kinase cascade controlling cell growth and differentiation. Activation of MEK1/2 occurs through phosphorylation of two

serine residues at position 217 and 221, also in the L12 loop of subdomain VIII by Raf-like molecules. p38 MAPK and MEK1/2 may share the same upstream signaling.

p85 and $p66^{Shc}$ were undetectable in $HSY_{R2\text{-}IIIb}$ and SGE, suggesting that the upstream signaling of p38 and MEK1/2 were partially blocked in both cells.

It has been well established that among the six to eight sequential components of this cascade, only p42 and p44 MAPKs, the most downstream elements, possess the unique potential to shuttle between the cytoplasm and the nucleus (Boulton, T. G. 1991, Jaaro, H. 1997). The p38 MAPK-nuclear translocation was observed in HSYzeo cells in present study. In resting cells, p38 MAPK was localized in the cytoplasm, probably via a cytoplasmic anchoring complex. How p38 MAPK dissociate from the cytoplasmic anchoring complex upon activation and how enter to the nucleus are not entirely understood in the present study. However, some observations on ERK might provide a little of hints. One interesting idea proposed by Seger's group (Jaaro, H., 1997) is that upon serum stimulation, the MEK-p42/p44 MAPK complex translocates to the nucleus where, following dissociation, only MEK is rapidly excluded via its active nuclear export signal sequence. Subsequent to this dissociation, p42/p44 MAPK could easily translocate to the nucleus via simple diffusion, although a co-transport involving association of p42/p44 MAPK with their NLS-containing substrates cannot be excluded.

The mechanism of p38 MAPK nuclear translocation and the activities of p38 MAPK nuclear accumulation is not clear. It was speculated that, signals that trigger the nuclear accumulation of p38 MAPK may be mitogenic one, because the growth rate of HSYzeo was inhibited by p38 MAPK specific inhibitor SB203580 (data not show), which can impede the nuclear

translocation of p38 MAPK, although the effect of the inhibitor on the apoptosis in HSYzeo has not been studied yet. SEK/MKK3/ MKK6-p38 MAPK complex might be dissociated by the unidentified element and p38 MAPK translocate into nuclear and become one part of mitogenic activator. If the element which promote the dissociation of MKK3 / MKK6-p38 MAPK complex were identified, the inhibitor for the elements will be another adenocarcinoma supressor.

These results suggested that KGFR/FGFR2-IIIb expression or signal could dominantly suppress both p38 phosphorylation and nuclear translocation in HSYzeo stimulated by FGFR1 signal, and induce apoptosis and differentiation.

Chapter 3 *Ex vivo* gene transfer of KGFR/FGFR2-IIIb gene into xenografted tumor cells

1. Introduction

Human malignant salivary gland tumors are highly aggressive neoplasms that readily invade adjacent tissues and metastase to distant organs at early stages of the disease (Kurokawa, R. 1989). Efficient therapeutic approaches at early stage are needed to be explored. As described in chapter 1 and 2, KGFR/FGFR2-IIIb gene induced differentiation and apoptosis in HSY cells *in vitro* and *in vivo*. These results strongly suggest the possibility that FGFR2-IIIb gene therapy could be a good alternative to treat malignant salivary gland tumors.

Rapid progress in molecular biology has made it possible to transfer any genes of interest to target tissues of living animals. Currently, most efforts toward postnatal gene therapy have relied on indirect means of introducing new genetic information into tissues: target cells are removed from the body, infected with viral vectors carrying the new genetic information, and then reimplanted into body (Leddley, F.D. 1989). The success of gene therapy requires a safe and effective way to introduce the therapeutic gene into the tissues.

The method using adenoviral vectors can introduce foreign genes into differentiated non-dividing cells in living animal tissues (Akli, S. 1993, Bajocchi, G. 1993, le Gal La Salle, 1993, Ragot, T. 1993, Morris Jr. 1994, Mallet, J. 1994, Mah, C. 1998). However, the preparation of recombinant viral granules is cumbersome, and the efficiency of recombinant formation is

sometimes very low. Moreover, the foreign genes introduced with adenoviral vectors are not integrated into the genomic DNAs of the host cells, since they are simple to construct and integrate the foreign genes efficiently into host genome. Such vectors, however, can infect only propagating cells and are inactivated by complements in the blood stream (Mulligan, R.C, 1993). Therefore, the practical application of these vectors for *in vivo* transfection is considerably restricted.

As for the non-viral delivery of DNA, lipofection with cationic liposomes associated with anionic plasmid DNA was shown to deliver foreign genes efficiently into cells *in vitro*, and recently *in vivo* by endocytotic machinery (Williams, R. S. 1991, Dzau, V.J. 1996). Endocytosed plasmid DNAs are, however, liable to be digested in the lysosome, and cationic liposomes have some cytotoxicity (Mulligan,R. C. 1993). A particle-gun powered either by high-pressure gas or by a gunpowder explosion successfully introduced metallo-particles coated with foreign plasmid DNAs into living cells. Recently, a handy particle-gun that does not require a decompression chamber was developed, making the direct gene transfer into living animal cells much easier (Sundaram, P. 1996). With this technique, however, metallo-particles only reach the cells on the surface of organs. Therefore, the target cells must be exposed by surgical operation, and this technique seems to be useful in only restricted tissues.

Electroporation (EP) efficiently introduces foreign genes into living cell, but the use of this technique had been restricted to suspensions of cultured cells only, since the electric pulses are administered in a cuvette-type electrode. Recently, various types of electrodes have been developed, and electroinjection of chemicals or foreign genes was applied *in vivo* (Belehradek, M. 1993, Heller, R. 1996, Nishi, T. 1996, Muramatsu, T. 1998). Although the *in*

vitro EP with a cuvette-type electrode is carried out with an electric pulse at several kilovolts for several microseconds, multiple pulses under much lower voltage for several milliseconds are used for *in vivo* EP. The methods of such *in vivo* and *ex vivo* gene transfer for either therapeutic or experimental purposes largely rely on viral vectors. Hence, EP has been found to be efficient *in vivo* in deep tissues of living animals. Recently, however, depth-targeted gene delivery into skin was demonstrated in mice, which would allow to treat skin cancers with an improved effect when used with tumor-suppressor genes such as p53. In the rat brain tumor, local expression of the human monocyte chemo-attractant protein-1 cDNA was transferred by *in vivo* EP. The presence of large numbers of macrophages and lymphocytes observed in the treated tumor tissues indicates potential of *in vivo* EP for gene therapy of brain cancer.

For researchers, an easy, safe, non-toxic, and possibly efficient delivery of genes to a specified target tissue has been an attractive issue, and clinical application is the goal for every basic research.

In this chapter, I have tried to electro-gene transfer of KGFR gene by *ex vivo* EP (KGFR gene therapy) into HSY-derived adenocarcinomas of living athymic nude mice. The efficiency of electro-gene transfer and the effect of KGFR gene therapy against tumor growth were studied.

2. Materials and methods

2.1. Experimental conditions for EP

Electric pulses were generated with an Electro Square Porator (BTX ECM2001M). The pulses were given to tumor tissues by a pair of needle-type electrode (Meiwa Shoji, Tokyo, Japan) which were inserted subcutaneously around the tumors. Electric pulses were 50 m sec in duration at 50 or 70 voltage. The resistance was monitored with a graphic pulse analyzer (MVC540R).

2.2 Electric gene transfer

HSY(2×10^6 cells) was inoculated to 6-week-old male athymic mice subcutaneously. At 1, 2, 3 and 4 weeks after the inoculation, pcDNA3.1/zeo-KGFR/FGFR2-IIIb or pcDNA3.1/zeo (empty) vector was electro-transferred to transplanted tumors as follow. The mice were anesthetized with diethyl ether. The needle-type electrodes were inserted subcutaneously around the tumor (Fig. 22), and electric resistance was measured. The plasmid DNA (50μg) in 50μl of PBS was injected into the center of tumor with 27 gauge needle. Immediately after the DNA injection, electric pulses were administered. Electric resistance of the tumors were measured once again just after the electric administration. The size of subcutaneous tumors was externally measured periodically in two dimensions using venire calipers at indicated times. Mice were sacrificed at 48 h, 1, 2, 3 and 4 weeks after EP. Tumor specimen were fixed in 4% PFA and embedded in paraffin for histological examination and immunohistochemical examination with Anti-FGFR2 antibody (Santa Crutz

Biotechnology, Inc. USA). All of the animal procedures were in accordance with guideline of the institutional animal care committee of Hiroshima University.

3. Results

3.1. Ex vivo KGFR gene transfer inhibits the tumor growth

At 1 week after HSY cell inoculation, KGFR gene was electro-transfered into the tumors. The size of tumors became smaller within 1 week after EP and then disappeared (Fig.23). At 4 weeks after HSY cell inoculation, the growth rate of tumors electro-transfered by KGFR gene was inhibited significantly, but none of tumor was disappeared. On the other hand, the tumors electro-transferred with empty vector at 1 or 4 weeks after inoculation grew well (Fig.24).

3.2. KGFR/FGFR2-IIIb gene product constantly expressed in adenocarcinomas for at least 4 weeks after EP

To study the efficacy of electro-gene transfer, anti-FGFR2 antibody (anti-bek) was used to detect expression of KGFR protein in the tumors by immunohistchemical analysis.

Forty eight hours after gene transfer, about 70% of tumor cells exhibited KGFR expression in the nucleus and cytoplasm (Fig.25A). Two-three weeks after gene transfer, about 20% of tumor cells still express KGFR in the cytoplasm and cell membranes (Fig.25B and 25C).

Moreover, KGFR was intensely immuopositive in fibroblasts suggesting that KGFR gene was transfered not only to tumor cells but also to fibroblasts in stromas.

3.3. Histological evaluation

In some areas of tumors, the cytoplasm of tumor cells expressing KGFR were clear, and the ratio of nucleus to cytoplasm is very low. In the other areas of tumors, epithelial compartment and stroma compartment were well defined, but duct-like structure was very rare. In addition, KGFR-expressing tumor cells were also TUNEL positive (Fig.26).

4. Discussion

In this chapter, I have successfully treated salivary gland adenocarcinomas in athymic nude mice with KGFR/FGFR2-IIIb gene therapy by using electro-gene transfer.

KGFR/FGFR2-IIIb gene might be electro-transfered into at least three kinds of cells: tumor cells, fibroblasts and epithelial cells. As discussed in chapter 1, when KGFR/FGFR2-IIIb gene was transferred into the tumor cells, the communication to stroma was recovered. When KGFR/FGFR2-IIIb gene was transferred into fibroblasts, fibroblasts would be stimulated by KGF secreted by itself, and proliferation of fibroblasts was promoted. This is the reason why there is sufficient stroma components in KGFR/FGFR2-IIIb transfected tissues. As epithelial cell pocesses FGFR2 gene, when KGFR/FGFR2-IIIb gene was transferred into epithelial cells, the proliferation of epithelial cells could be also promoted.

According to the previous studies, at low voltage, the plasma membranes of cells are not sufficiently altered to allow passage of DNA molecules, while at higher voltages the cells are irreversibly damaged (Sambrook, J. 1989). Many studies indicated that the maximal levels of transient gene expression are reached between 250V-750V/cm with single electric pulse lasting for 20-100 msec.

According to my preliminary experiments, if tumors were treated with 100 voltage, 100 m sec and 8 pulses with empty vector, 30% of the tumor tissues was necrotized (data are not shown) and if maintain the duration in 50 m sec and the voltage around 50-70 V according to electric resistance, transfer efficiency would be the best without severe cell damage.

It is reported that efficacy of electro-transfer was dependent on the

of DNA injected into the tissue. Heller et al (1996) used three pairs of electrodes, which consisted of six needles arrayed at even intervals around a 1 cm diameter circle, and six pulse were administered with rotation of the pairs and direction of the electrodes. An apparent maximum expression of the marker gene was observed when 25μg of plasmid DNA was injected, which stands in marked contrast to the dose-dependent increase in the efficiency of electro-transfer. Suzuki et al (1998) reported that rat liver lobe was sandwitched between a pair of electrode disks, and 8 pulses were administered. When only 1μg of DNA was injected, a small amount of expression signal was observed. The sizes of the signal dots were larger when 20μg of plasmid DNA was injected, and the intensity of each signal dot increased drastically with the 40-80μg injection. In the present study, the tumors were arrayed by a pair of needle-type electrode. This type of electrode is considered to be appropriate to subcutaneous tumor. Furthermore, 8 pulse were administered with the same electric current direction per electroporation. This shapes of the electric field and the effects of eletrophoresis on the injected DNA might be different from the other methods. First, the shape of current was square which can remain a long tail of current, and the electric power is mild and enduring, which might recovered cell from damage of electroporation very quickly. Second, current direction was fixed, and this fixed current direction limited DNA electrophoresis. If the current direction was rotated, the electro-transfer efficiency would be better. The rotation was given up because of thinking over the damage to animal skin. Because electric current may make heat that can degrade DNA and injure the tissue, the chilled DNA solution may protect both DNA and tissue from heat damage.

Besides the transfer efficiency of KGFR gene, a critical concern is whether the expression of KGFR gene is properly regulated *in vivo* as expected.

Several questions may be raised to the behavior of transferred genes by *in vivo* EP; how long does KGFR gene expression last? Is the tissue- or cell-specific gene expression maintained? Is the gene expression induced as intended?

The duration of gene expression after *in vivo* EP depends on the target tissue and probably to some extent on the plsmid construct. Previous studies indicated that lacZ reporter gene expression was maintained for at least 21 days in rat liver after EP (Heller, R. 1996). In present study, KGFR expresseion last at least 4 weeks after *in vivo* EP. Another factor that affect EP efficiency, not entirely, is the type of electrode. Although there are several reports of EP by using pincette-type electrode, in present study, needle-type electrode were used which gives a expective results.

If muscles are target site, the duration of gene expression would be longer than that in any other tissues. In the rat abdominal muscle, luciferase expression was maintained at least 1 mouth (Tripathy, S. K. 1996). Therefore, for gene therapy where long-term gene expression is desired, application of *in vivo* EP to muscles would offer a good chance for supplying therapeutic proteins that are synthesized and secreted in the blood circulation. In present study, 4 weeks after EP, the expression of KGFR gene in the tumor were still observed.

In the present study, I discussed the characteristics of *in vivo* EP which is rather unpopular means of nonviral gene transfer. Studies with EP contribute only to about 1% of the total *in vivo* gene transfer and gene therapy experiments. Despite of its unpopularity at present, i*n vivo* EP might be more extensively used in near future as it is easy, safe, and non-toxic.

A specific feature of *in vivo* EP compared with other nonviral gene transfer methods is the use of electrodes that must be placed along target sites.

Although gene transfer procedure of EP, i.e. electric pulse application, is done quickly within a matter of second, placing electrodes of the correct size and in an adequate way is sometimes difficult when the target site is located deep in the body or spread throughout the body. A further appraisal of EP as a nonviral means of gene transfer should be brought forth in the future after more detailed analyses are made from a view point of both experimental and therapeutic purpose.

In this chapter, I have successfully proved that EP might be one of the best method to deliver external gene into living tissues/cells, and shown that KGFR expression suppresses the growth and induces differentiation/apoptosis in HSY tumors.

These results strongly suggested that KGFR gene therapy by using EP might be a good alternative to cure malignant salivary tumors.

Conclusion

In the present study, it have been demonstrated that the expression of wild-type KGFR/FGFR2-IIIb in human salivary gland-derived adenocarcinomas resulted in a significant inhibition of tumor growth and induction of differentiation/apoptosis *in vitro*, *in vivo* and *ex vivo*.

The anti-oncogenic effect that resulted from KGFR/FGFR2-IIIb overexpression is acompanied with apoptotic cell death, decreased cell proliferation and local cellular differentiation. Moreover, the inhibition of phosphorylation of p38 MAPK, p85 and $p66^{shc}$ might indirectly inhibit the proliferation and promote differentiation of the tumor cells.

All of these properties confirm the potential of KGFR/FGFR2-IIIb gene transfer as a new strategy of gene therapy for human salivary gland adenocarcinomas. Whether *in vivo* or *ex vivo* gene transfer should be applied remains to be established and experimentally tested. However, regarding the local antitumor effects obtained by KGFR gene therapy, it is strongly suggested that this therapeutic approach appears promising for adjuvant treatment of both early and late stage of adenocarcinomas.

References

Akli, S., Caillaud, C., Vigne, E., Stratford Perricaudet, L.D., Poenaru, L., Perricaudet, M., Kahn, A. and Peschanski, M.R., Transfer of a foreign gene into the brain using adenovirus vectors. *Nat Genet*, **3,** 224-8 (1993).

Bajocchi, G., Feldman, S.H., Crystal, R.G. and Mastrangeli, A., Direct in vivo gene transfer to ependymal cells in the central nervous system using recombinant adenovirus vectors . *Nat Genet*, **3,** 229-34 (1993).

Barry, M.A., Behnke, C.A. and Eastman, A., Activation of programmed cell death (apoptosis) by cisplatin, other anticancer drugs, toxins and hyperthermia. *Biochem Pharmacol*, **40,** 2353-62 (1990).

Batzer, A.G., Rotin, D., Urena, J.M., Skolnik, E.Y. and Schlessinger, J., Hierarchy of binding sites for Grb2 and Shc on the epidermal growth factor receptor. *Mol-Cell-Biol*, **14,** 5192-201 (1994).

Belehradek, M., Domenge, C., Luboinski, B., Orlowski, S., Belehradek, J., Jr. and Mir, L.M., Electrochemotherapy, a new antitumor treatment. First clinical phase I-II trial. *Cancer*, **72,** 3694-700 (1993).

Bottaro, D.P., Rubin, J.S., Ron, D., Finch, P.W., Florio, C. and Aaronson, S.A., Characterization of the receptor for keratinocyte growth factor. Evidence for multiple fibroblast growth factor receptors. *J Biol Chem*, **265,** 12767-70 (1990).

Boulton, T.G., Nye, S.H., Robbins, D.J., Ip, N.Y., Radziejewska, E.,

Morgenbesser, S.D., DePinho, R.A., Panayotatos, N., Cobb, M.H. and Yancopoulos, G.D., ERKs: a family of protein-serine/threonine kinases that are activated and tyrosine phosphorylated in response to insulin and NGF. *Cell*, **65,** 663-75 (1991).

Burgess, W.H., Shaheen, A.M., Ravera, M., Jaye, M., Donohue, P.J. and Winkles, J.A., Possible dissociation of the heparin-binding and mitogenic activities of heparin-binding (acidic fibroblast) growth factor-1 from its receptor-binding activities by site-directed mutagenesis of a single lysine residue. *J Cell Biol*, **111,** 2129-38 (1990).

Clark, S.G., Stern, M.J. and Horvitz, H.R., C. elegans cell-signalling gene sem-5 encodes a protein with SH2 and SH3 domains. *Nature*, **356,** 340-4 (1992).

Coughlin, S.R., Barr, P.J., Cousens, L.S., Fretto, L.J. and Williams, L.T., Acidic and basic fibroblast growth factors stimulate tyrosine kinase activity in vivo. *J Biol Chem*, **263,** 988-93 (1988).

Crawley, J.B., Rawlinson, L., Lali, F.V., Page, T.H., Saklatvala, J. and Foxwell, B.M., T cell proliferation in response to interleukins 2 and 7 requires p38MAP kinase activation. *J Biol Chem*, **272,** 15023-7 (1997).

Cuenda, A., Cohen, P., Buee Scherrer, V. and Goedert, M., Activation of stress-activated protein kinase-3 (SAPK3) by cytokines and cellular stresses is mediated via SAPKK3 (MKK6); comparison of the specificities of SAPK3 and SAPK2 (RK/p38). *EMBO J*, **16,** 295-305 (1997).

Derijard, B., Hibi, M., Wu, I.H., Barrett, T., Su, B., Deng, T., Karin, M. and Davis, R.J., JNK1: a protein kinase stimulated by UV light and Ha-Ras that binds and phosphorylates the c-Jun activation domain. *Cell*, **76,** 1025-37 (1994).

Dzau, V.J., Mann, M.J., Morishita, R. and Kaneda, Y., Fusigenic viral liposome for gene therapy in cardiovascular diseases . *Proc Natl Acad Sci U S A*, **93,** 11421-5 (1996).

Emoto, H., Tagashira, S., Mattei, M.G., Yamasaki, M., Hashimoto, G., Katsumata, T., Negoro, T., Nakatsuka, M., Birnbaum, D., Coulier, F. and Itoh, N., Structure and expression of human fibroblast growth factor-10. *J Biol Chem*, **272,** 23191-4 (1997).

Eriksson, A.E., Cousens, L.S., Weaver, L.H. and Matthews, B.W., Three-dimensional structure of human basic fibroblast growth factor. *Proc Natl Acad Sci U S A*, **88,** 3441-5 (1991).

Finch, P.W., Rubin, J.S., Miki, T., Ron, D. and Aaronson, S.A., Human KGF is FGF-related with properties of a paracrine effector of epithelial cell growth. *Science*, **245,** 752-5 (1989).

Foltz, I.N., Lee, J.C., Young, P.R. and Schrader, J.W., Hemopoietic growth factors with the exception of interleukin-4 activate the p38 mitogen-activated protein kinase pathway. *J Biol Chem*, **272,** 3296-301 (1997).

Fukuda, M., Gotoh, Y. and Nishida, E., Interaction of MAP kinase with MAP kinase kinase: its possible role in the control of nucleocytoplasmic transport of

MAP kinase. *EMBO J*, **16,** 1901-8 (1997).

Gale, N.W., Kaplan, S., Lowenstein, E.J., Schlessinger, J. and Bar Sagi, D., Grb2 mediates the EGF-dependent activation of guanine nucleotide exchange on Ras. *Nature*, **363,** 88-92 (1993).

Gavrieli, Y., Sherman, Y. and Ben Sasson, S.A., Identification of programmed cell death in situ via specific labeling of nuclear DNA fragmentation. *J Cell Biol*, **119,** 493-501 (1992).

Gemel, J., Gorry, M., Ehrlich, G.D. and MacArthur, C. A., Sructures and sequence of human FGF-8. *Genomics*, **35,** 253-7 (1996).

Goedert, M., Cuenda, A., Craxton, M., Jakes, R. and Cohen, P., Activation of the novel stress-activated protein kinase SAPK4 by cytokines and cellular stresses is mediated by SKK3 (MKK6); comparison of its substrate specificity with that of other SAP kinases. *EMBO J*, **16,** 3563-71 (1997).

Graeber, T.G., Osmanian, C., Jacks, T., Housman, D.E., Koch, C.J., Lowe, S.W. and Giaccia, A.J., Hypoxia-mediated selection of cells with diminished apoptotic potential in solid tumours . *Nature*, **379,** 88-91 (1996).

Hadari, Y.R., Kouhara, H., Lax, I. and Schlessinger, J., Binding of Shp2 tyrosine phosphatase to FRS2 is essential for fibroblast growth factor-induced PC12 cell differentiation. *Mol Cell Biol*, **18,** 3966-73 (1998).

Han, J., Lee, J.D., Bibbs, L. and Ulevitch, R.J., A MAP kinase targeted by

endotoxin and hyperosmolarity in mammalian cells. *Science*, **265,** 808-11 (1994).

Hattori, Y., Yamasaki, M. and Itoh, N., The rat FGF-5 mRNA variant generated by alternative splicing encodes a novel truncated from of FGF-5. *Biochim Biophys Acta,* **1306,** 31-3 (1996).

He, J., Whitacre, C.M., Xue, L.Y., Berger, N.A. and Oleinick, N.L., Protease activation and cleavage of poly(ADP-ribose) polymerase: an integral part of apoptosis in response to photodynamic treatment. *Cancer Res*, **58,** 940-6 (1998).

Heldin, C.H., Dimerization of cell surface receptors in signal transduction. *Cell*, **80,** 213-23 (1995).

Heller, R., Jaroszeski, M., Atkin, A., Moradpour, D., Gilbert, R., Wands, J. and Nicolau, C., In vivo gene electroinjection and expression in rat liver. *FEBS Lett*, **389,** 225-8 (1996).

Hou, J.Z., Kan, M.K., McKeehan, K., McBride, G., Adams, P. and McKeehan, W.L., Fibroblast growth factor receptors from liver vary in three structural domains. *Science*, **251,** 665-8 (1991).

Hou, J., Kan, M., Wang, F., Xu, J.M., Nakahara, M., McBride, G., McKeehan, K. and McKeehan, W.L., Substitution of putative half-cystine residues in heparin-binding fibroblast growth factor receptors. Loss of binding activity in both two and three loop isoforms. *J Biol Chem*, **267,** 17804-8 (1992).

Houssaint, E., Blanquet, P.R., Champion Arnaud, P., Gesnel, M.C., Torriglia, A., Courtois, Y. and Breathnach, R., Related fibroblast growth factor receptor genes exist in the human genome. *Proc Natl Acad Sci U S A*, **87,** 8180-4 (1990).

Imamura, T., Tokita, Y. and Mitsui, Y., Purification of basic FGF receptors from rat brain. *Biochem Biophys Res Commun*, **155,** 583-90 (1988).

Jaaro, H., Rubinfeld, H., Hanoch, T. and Seger, R., Nuclear translocation of mitogen-activated protein kinase kinase (MEK1) in response to mitogenic stimulation. *Proc Natl Acad Sci U S A*, **94,** 3742-7 (1997).

Jaye, M., Schlessinger, J. and Dionne, C.A., Fibroblast growth factor receptor tyrosine kinases: molecular analysis and signal transduction. *Biochim Biophys Acta*, **1135,** 185-99 (1992).

Jiang, Y., Chen, C., Li, Z., Guo, W., Gegner, J.A., Lin, S. and Han, J., Characterization of the structure and function of a new mitogen-activated protein kinase (p38 beta). *J Biol Chem*, **271,** 17920-6 (1996).

Johnson, D.E., Lu, J., Chen, H., Werner, S. and Williams, L.T., The human fibroblast growth factor receptor genes: a common structural arrangement underlies the mechanisms for generating receptor forms that differ in their third immunoglobulin domain. *Mol Cell Biol*, **11,** 4627-34 (1991).

Kan, M., Shi, E.G. and McKeehan, W.L., Identification and assay of fibroblast

growth factor receptors. *Methods Enzymol*, **198,** 158-71 (1991).

Kerr, J.F., Winterford, C.M. and Harmon, B.V., Apoptosis. Its significance in cancer and cancer therapy. *Cancer*, **73,** 2013-26 (1994).

Kobrin, M.S., Yamanaka, Y., Friess, H., Lopez, M.E. and Korc, M., Aberrant expression of type I fibroblast growth factor receptor in human pancreatic adenocarcinomas. *Cancer Res*, **53,** 4741-4 (1993).

Kouhara, H., Hadari, Y.R., Spivak Kroizman, T., Schilling, J., Bar Sagi, D., Lax, I. and Schlessinger, J., A lipid-anchored Grb2-binding protein that links FGF-receptor activation to the Ras/MAPK signaling pathway. *Cell*, **89,** 693-702 (1997).

Kurada, P. and White, K., Ras promotes cell survival in Drosophila by downregulating hid expression . *Cell*, **95,** 319-29 (1998).

Kurokawa, R., Kyakumoto, S. and Ota, M., Autocrine growth factor in defined serum-free medium of human salivary gland adenocarcinoma cell line HSG. *Cancer Res*, **49,** 5136-42 (1989).

Kyriakis, J.M., Banerjee, P., Nikolakaki, E., Dai, T., Rubie, E.A., Ahmad, M.F., Avruch, J. and Woodgett, J.R., The stress-activated protein kinase subfamily of c-Jun kinases. *Nature*, **369,** 156-60 (1994).

Lamb, K., Rosfjord, E., Brigman, K. and Rizzino, A., Binding of transcription factors to widely-separated cis-regulatory elements of the murine FGF-4 gene.

Mol Reprod Dev, **44,** 460-71 (1996).

Laster, S.M., Wood, J.G. and Gooding, L.R., Tumor necrosis factor can induce both apoptic and necrotic forms of cell lysis. *J Immunol*, **141,** 2629-34 (1988).

Le Gal La Salle, G., Robert, J.J., Berrard, S., Ridoux, V., Stratford Perricaudet, L.D., Perricaudet, M. and Mallet, J., An adenovirus vector for gene transfer into neurons and glia in the brain. *Science*, **259,** 988-90 (1993).

Lechner, C., Zahalka, M.A., Giot, J.F., Moller, N.P. and Ullrich, A., ERK6, a mitogen-activated protein kinase involved in C2C12 myoblast differentiation. *Proc Natl Acad Sci U S A*, **93,** 4355-9 (1996).

Lee, P.L., Johnson, D.E., Cousens, L.S., Fried, V.A. and Williams, L.T., Purification and complementary DNA cloning of a receptor for basic fibroblast growth factor. *Science*, **245,** 57-60 (1989).

Lenormand, P., Brondello, J.M., Brunet, A. and Pouyssegur, J., Growth factor-induced p42/p44 MAPK nuclear translocation and retention requires both MAPK activation and neosynthesis of nuclear anchoring proteins. *J Cell Biol*, **142,** 625-33 (1998).

Li, N., Batzer, A., Daly, R., Yajnik, V., Skolnik, E., Chardin, P., Bar Sagi, D., Margolis, B. and Schlessinger, J., Guanine-nucleotide-releasing factor Sos1 binds to Grb2 and links receptor tyrosine kinases to Ras signalling. *Nature*, **363,** 85-8 (1993).

Lowenstein, E.J., Daly, R.J., Batzer, A.G., Li, W., Margolis, B., Lammers, R., Ullrich, A., Skolnik, E.Y., Bar Sagi, D. and Schlessinger, J., The SH2 and SH3 domain-containing protein GRB2 links receptor tyrosine kinases to ras signaling. *Cell*, **70,** 431-42 (1992).

Lu, C. and Tanigawa, N., Spontaneous apoptosis is inversely related to intratumoral microvessel density in gastric carcinoma. *Cancer Res*, **57,** 221-4 (1997).

Mah, C., Qing, K., Khuntirat, B., Ponnazhagan, S., Wang, X.S., Kube, D.M., Yoder, M.C. and Srivastava, A., Adeno-associated virus type 2-mediated gene transfer: role of epidermal growth factor receptor protein tyrosine kinase in transgene expression. *J Virol*, **72,** 9835-43 (1998).

Mallet, J., Le Gal La Salle, G., Robert, J.J., Berrard, S., Ridoux, V., Stratford Perricaudet, L.D. and Perricaudet, M., Adenovirus mediated gene transfer to the central nervous system. *Gene Ther*, **1 Suppl 1,** S52 (1994).

Marics, I., Adelaide, J., Raybaud, F., Mattei, M. G., Goalier, F., Planche, J., deLapsyriere, O. and Birnbaum, D., Characterization of the HST-related FGF 6 gene, a new member of the fibroblast growth factor family. *Oncogene*, **4,** 335-40 (1989).

Marshall, C.J., Specificity of receptor tyrosine kinase signaling: transient versus sustained extracellular signal-regulated kinase activation. *Cell*, **80,** 179-85 (1995).

Mason, I.J., The ins and outs of fibroblast growth factors. *Cell*, **78,** 547-52 (1994).

Miki, T., Fleming, T.P., Bottaro, D.P., Rubin, J.S., Ron, D. and Aaronson, S.A., Expression cDNA cloning of the KGF receptor by creation of a transforming autocrine loop. *Science*, **251,** 72-5 (1991).

Miyamoto, M., Naruo, K., Seko, C., Matsumoto, S., Kondo, T. and Kurokawa, T., Molecular cloning of a novel cytokine cDNA encoding the ninth member of the fibroblast growth factor family, which has a unique secretion property. *Mol Cell Biol*, **13,** 4251-9 (1993).

Morris, B.D., Jr., Drazan, K.E., Csete, M.E., Werthman, P.E., Van Bree, M.P., Rosenthal, J.T. and Shaked, A., Adenoviral-mediated gene transfer to bladder in vivo. *J Urol*, **152,** 506-9 (1994).

Mulligan, R.C., The basic science of gene therapy. *Science*, **260,** 926-32 (1993).

Murakami, A., Grinberg, D., Thurlow, J. and Dickson, C., Identification of positive and negative regulatory elements involved in the retinoic acid/cAMP induction of FGF-3 transcription in F9 cells. *Nucleïc Acids Res*, **21,** 5351-9 (1993).

Muramatsu, T., Nakamura, A. and Park, H.M., In vivo electroporation: a powerful and convenient means of nonviral gene transfer to tissues of living animals (Review). *Int J Mol Med*, **1,** 55-62 (1998).

Myoken, Y., Myoken, Y., Okamoto, T., Kan, M., Sato, J.D. and Takada, K., Release of fibroblast growth factor-1 by human squamous cell carcinoma correlates with autocrine cell growth. *In Vitro Cell Dev Biol Anim*, **30a,** 790-5 (1994).

Myoken, Y., Myoken, Y., Okamoto, T., Sato, J.D., Takada, K., Myoken, Y., Myoken, Y., Okamoto, T., Sato, J.D., Kan, M., McKeehan, W.L., Fujihara, M. and Takada, K., Effect of fibroblast growth factor-1 on the three-dimensional growth and morphogenesis of human salivary gland epithelial cells embedded in collagen gels. *In Vitro Cell Dev Biol Anim*, **31,** 84-6 (1995).

Myoken, Y., Myoken, Y., Okamoto, T., Sato, J.D., Kan, M., McKeehan, W.L., Nakahara, M. and Takada, K., Immunohistochemical study of overexpression of fibroblast growth factor-1 (FGF-1), FGF-2, and FGF receptor-1 in human malignant salivary gland tumours. *J Pathol*, **178,** 429-36 (1996).

Myoken, Y., Myoken, Y., Okamoto, T., Kan, M., McKeehan, W.L., Sato, J.D. and Takada, K., Expression of fibroblast growth factor-1 (FGF-1), FGF-2 and FGF receptor-1 in a human salivary-gland adenocarcinoma cell line: evidence of growth. *Int J Cancer*, **65,** 650-7 (1996).

Myoken, Y., Myoken, Y., Okamoto, T., Sato, J.D., Kan, M., McKeehan, W.L., Fujihara, M. and Takada, K., Immunohistochemical localization of fibroblast growth factor-1 (FGF-1), FGF-2 and fibroblast growth factor receptor-1 (FGFR-1) in pleomorphic adenoma of the salivary glands. *J Oral Pathol Med*, **26,** 17-22 (1997).

Okamoto, T., Myoken, Y., Yabumoto, M., Osaki, T., Fujita, Y., Whitney, R.G., Kan, M., Crabb, J.W., Sato, G.H., Kato, Y., Takada, K. and Sato, J.D., Androgen-dependent expression of fibroblast growth factor-1 in submaxillary gland of mouse. *Biochem Biophys Res Commun*, **221,** 795-802 (1996).

Plotnikov, A.N., Schlessinger, J., Hubbard, S.R. and Mohammadi, M., Structure basis for FGF receptor dimerization and activation. *Cell*, **98**, 641-50 (1999).

Ragot, T., Vincent, N., Chafey, P., Vigne, E., Gilgenkrantz, H., Couton, D., Cartaud, J., Briand, P., Kaplan, J.C., Perricaudet, M. and et al., Efficient adenovirus-mediated transfer of a human minidystrophin gene to skeletal muscle of mdx mice. *Nature*, **361,** 647-50 (1993).

Rausch, O. and Marshall, C.J., Tyrosine 763 of the murine granulocyte colony-stimulating factor receptor mediates Ras-dependent activation of the JNK/SAPK mitogen-activated protein kinase pathway. *Mol Cell Biol*, **17,** 1170-9 (1997).

Reitamo, S., Konttinen, Y.T. and Segerberg Konttinen, M., Distribution of lactoferrin in human salivary glands. *Histochemistry*, **66,** 285-91 (1980).

Ron, D., Bottaro, D.P., Finch, P.W., Morris, D., Rubin, J.S. and Aaronson, S.A., Expression of biologically active recombinant keratinocyte growth factor. Structure/function analysis of amino-terminal truncation mutants. *J Biol Chem*, **268,** 2984-8 (1993).

Rozakis Adcock, M., Fernley, R., Wade, J., Pawson, T. and Bowtell, D., The SH2 and SH3 domains of mammalian Grb2 couple the EGF receptor to the Ras activator mSos1. *Nature*, **363,** 83-5 (1993).

Rubin, J.S., Osada, H., Finch, P.W., Taylor, W.G., Rudikoff, S. and Aaronson, S.A., Purification and characterization of a newly identified growth factor specific for epithelial cells. *Proc Natl Acad Sci U S A*, **86,** 802-6 (1989).

Salcini, A. E., McGlade, J., Pelicci, G., Nicoletti, I., Pawson, T. and Pelicci, P. G., Formation of Shc-Grb2 complexes is necessary to induce neoplastic transformation by overexpression of Shc proteins. *Oncogene*, **9,** 2827-36 (1994).

Sato, M., Hayashi, Y., Yanagawa, T., Yoshida, H., Yura, Y., Azuma, M. and Ueno, A., Intermediate-sized filaments and specific markers in a human salivary gland adenocarcinoma cell line and its nude mouse tumors. *Cancer Res*, **45,** 3878-90 (1985).

Shiah, S.G., Chuang, S.E., Chau, Y.P., Shen, S.C. and Kuo, M.L., Activation of c-Jun NH2-terminal kinase and subsequent CPP32/Yama during topoisomerase inhibitor beta-lapachone-induced apoptosis through an oxidation-dependent pathway. *Cancer Res*, **59,** 391-8 (1999).

Suzuki, T., Shin, B.C., Fujikura, K., Matsuzaki, T. and Takata, K., Direct gene transfer into rat liver cells by in vivo electroporation. *FEBS-Lett*, **425,** 436-40 (1998).

Szebenyi, G. and Fallon, J.F., Fibroblast growth factors as multifunctional signaling factors. I*nter Review Cyto,* **185**, 45-106 (1999).

Thornberry, N.A., Rano, T.A., Peterson, E.P., Rasper, D.M., Timkey, T., Garcia Calvo, M., Houtzager, V.M., Nordstrom, P.A., Roy, S., Vaillancourt, J.P., Chapman, K.T. and Nicholson, D.W., A combinatorial approach defines specificities of members of the caspase family and granzyme B. Functional relationships established for key mediators of apoptosis. *J Biol Chem*, **272,** 17907-11 (1997).

Tripathy, S.K., Black, H.B., Goldwasser, E. and Leiden, J.M., Immune responses to transgene-encoded proteins limit the stability of gene expression after injection of replication-defective adenovirus vectors. *Nat Med*, **2,** 545-50 (1996).

Tripathy, S.K., Svensson, E.C., Black, H.B., Goldwasser, E., Margalith, M., Hobart, P.M. and Leiden, J.M., Long-term expression of erythropoietin in the systemic circulation of mice after intramuscular injection of a plasmid DNA vector. *Proc Natl Acad Sci U S A*, **93,** 10876-80 (1996).

Ullrich, A., Schlessinger, J., Barry, M.A., Behnke, C.A. and Eastman, A., Signal transduction by receptors with tyrosine kinase activity. *Cell*, **61,** 203-12 (1990).

Williams, R.S., Johnston, S.A., Riedy, M., DeVit, M.J., McElligott, S.G. and Sanford, J.C., Introduction of foreign genes into tissues of living mice by DNA-coated microprojectiles. *Proc Natl Acad Sci U S A*, **88,** 2726-30 (1991).

Xia, Z., Dickens, M., Raingeaud, J., Davis, R.J., Greenberg, M.E., Burgess, W.H., Shaheen, A.M., Ravera, M., Jaye, M., Donohue, P.J. and Winkles, J.A., Opposing effects of ERK and JNK-p38 MAP kinases on apoptosis. *Science*, **270,** 1326-31 (1995).

Yamasaki, M., Miyake, A., Tagashira, S. and Itoh, N., Structure and expression of the rat mRNA encoding a novel member of the fibroblast growth factor family. *J Biol Chem*, **271,** 15918-21 (1996).

Zhang, J.D., Cousens, L.S., Barr, P.J. and Sprang, S.R., Three-dimensional structure of human basic fibroblast growth factor, a structural homolog of interleukin 1 beta . *Proc Natl Acad Sci U S A*, **88,** 3446-50 (1991).

Figure legends

Fig. 1. Structure of wild-type KGFR/FGFR2-IIIb and its expression vector.

Fig. 2. Northern and Southern blot analysis for the expression of KGFR/FGFR2-IIIb mRNA in HSY, HSYzeo and HSY$_{R2\text{-}IIIb}$.

Expression of FGFR2-IIIb mRNA in HSY$_{R2\text{-}IIIb}$ was determined by Northern hybridization (**A**) and PCR-Southern hybridization (**B**) with [^{32}P]-labeled FGFR2-IIIb cDNA probe. The position and amount of rRNA 18S and 28S are indicated on the right side. FGFR2-IIIb was expressed in the HSY$_{R2\text{-}IIIb}$ but not in HSY and HSYzeo.

Fig. 3. Phase-contrast appearance of HSYzeo and HSY$_{R2\text{-}IIIb}$.

HSY$_{R2\text{-}IIIb}$ exhibited a cobble stone-like epithelial monolayer with strong intercellular interactions. HSYzeo exhibited a polygonal appearance but more rounded with less intercellular interactions.

Fig.4. Growth of HSY, HSYzeo and HSY$_{R2\text{-}IIIb}$ in serum-free culture.

Both HSY and HSYzeo cells proliferate well in serum-free RD5F at the doubling time of 16-18 hours whereas HSY$_{R2\text{-}IIIb}$ clones proliferate very slowly at the doubling time of 52-68 hours.

Fig. 5. Effects of FGFs on the growth of HSYzeo and HSY$_{R2\text{-}IIIb}$ in serum-free culture.

FGF-1 and FGF-2 at 20 ng/ml showed a 5-fold stimulation of HSYzeo cell growth in serum-free culture. None of FGFs stimulated the growth of HSY$_{R2\text{-}IIIb}$.

Fig. 6. Immunoperoxidase staining for α-amylase and lactoferrin proteins in HSYzeo and HSY$_{R2\text{-}IIIb}$.

HSYzeo exhibited weakly positive staining for α-amylase (**A**) and lactoferrin (**C**). HSY$_{R2\text{-}IIIb}$ showed intensive positive staining for α-amylase (**B**) and lactoferrin (**D**) in the cytoplasm and perinuclear regions. Scale bar: 20 μm

Fig. 7. Semi-quantitative RT-PCR analysis for α-amylase mRNA in HSY, HSYzeo , HSY$_{R2\text{-}IIIb}$ and SGE.

α-amylase mRNA was expressed in HSY$_{R2\text{-}IIIb}$ and SGE compared to HSYzeo. The band corresponding 230 bp are indicated. PCR amplification were carried out for 10, 20 and 30 cycles. **1**, negative control, **2**, HSY, **3**, HSYzeo, **4**, HSY$_{R2\text{-}IIIb}$, **5**, SGE.

Fig. 8. Trypan blue dye exclusion assay.

Trypan blue staining in HSYzeo and HSY$_{R2\text{-}IIIb}$. HSY$_{R2\text{-}IIIb}$ (**A**, **B**) and HSYzeo (**C**) were cultured with 20 ng/ml KGF in serum-free RD (-) for indicated periods. The cells were then harvested and spreaded in poly-L-lysine coated slides. Dead cells were stained deep blue color.

D, Cell survival (%) of HSY$_{R2\text{-}IIIb}$ and HSYzeo cultured with 20ng/ml KGF for indicated periods. Approximately, 10% of the cells has been died on day 2, 15% on day 3, 50% on day 4 and 90% on day 6, whereas HSYzeo continued to grow in the presence of KGF (20 ng/ml).

Fig. 9. Detection of Apoptosis in HSYzeo and HSY$_{R2\text{-}IIIb}$ with TUNEL staining and DNA fragmentation.

TUNEL method was used to detect the morphological evidences for apoptosis. TUNEL positive cells were observed in HSY$_{R2\text{-}IIIb}$ cultured for 1 day (**A**) and the percentage of the positive nuclei increased until 6 days of culture (**B**). No TUNEL positive cells were detected in HSYzeo (**C**).

D: No detectable DNA fragmentation was observed in HSY and HSYzeo cultured with KGF (20ng/ml) for 7 days. On the other hand, a typical DNA ladder was observed in HSY$_{R2\text{-}IIIb}$ cultured with KGF (20ng/ml) for 4 days, and was further increased over a 7 day-period.

Fig. 10. Immunofluorescent analysis of Caspase-3 (inactive form) in HSYzeo and HSY$_{R2\text{-}IIIb}$.

The inactive form of caspase-3 was highly expressed in HSYzeo **(A)**, but not in HSY$_{R2\text{-}IIIb}$ **(B)**.

Fluorometric Caspase-3 activity assay (**C**) shows that activity of Caspase-3 in HSY$_{R2\text{-}IIIb}$ was significantly higher than that in HSYzeo with or without KGF.

Fig. 11. The growth of HSY-, HSYzeo and HSY$_{R2\text{-}IIIb}$-derived tumors in athymic nude mice.

There was no significant difference between the tumor growth of HSYzeo and parental HSY. In contrast, there was a significant reduction in growth rate of HSY$_{R2\text{-}IIIb}$-derived tumors as compared with that of HSY- and HSYzeo-derived tumors. In addition, 24-3-9, 6-3-9, and 24-2-2 HSY$_{R2\text{-}IIIb}$ clones lost their tumorigenicities

Fig. 12. Macroscopic appearance of HSYzeo and HSY$_{R2\text{-}IIIb}$-derived tumors in athymic nude mice.

HSY- and HSYzeo-derived tumors exhibited irregularly rounded appearance with lobulated or multinodular surface. In contrast, the HSY$_{R2\text{-}IIIb}$-derived tumors was much smaller in size, softer and pale in comparison with HSYzeo tumors and exhibited rounded structures with smooth surface, and well encapsulated with and demarcated from the surrounding connective tissues.

Fig. 13. Histological evaluation of HSYzeo- and HSY$_{R2\text{-}IIIb}$-derived tumors in athymic nude mice.

A; Tumors developed from clone 2-4-2 exhibited predominant gland-like and acinar-like stuctures surrounded by stromal cells. Upon TUNEL examination, endogenous DNA fragmentation and apoptotic bodies were observed in the nuclei indicating apoptosis (arrow).

B; The histological appearances of HSYzeo-derived tumors exhibited typical adenocarcinomas with solid and trabecular pattern. The tumors were composed of cuboidal cells with occasional isocytism and mitosis. In addition, larger cells which had pale-staining eosinophilic cytoplasm were observed in some areas of the tumors.

Fig. 14. Detection of apoptotic DNA fragmentation in the HSYzeo and HSY$_{R2\text{-}IIIb}$ tumors by TUNEL staining.

Serial sections were stained with H&E (**A, C**) and TUNEL (**B, D**).

Endogenous DNA fragmentation and apoptotic bodies were observed in the nuclei of HSY$_{R2\text{-}IIIb}$ (**A, B**) (magnification, x400), but not in HSYzeo (**C, D**) (magnification: x200). Nuclei incdicating DNA fragmentation were stained brown (arrow).

Fig.15. Western blotting analysis for the phosphorylated proteins in HSYzeo and HSY$_{R2\text{-}IIIb}$.

The cell lysates extracted from HSYzeo and HSY$_{R2\text{-}IIIb}$ were immunoprecipated with anti-Grb2 antibody and were blotted with anti-phosphotyrosine antibody.

In HSYzeo, three of Grb2-associated proteins (p46^{shc}, p52^{shc}, p66^{shc}) and FRS2 were identified as tyrosine phosphorylated proteins. However, only p46^{shc} and p52^{shc} were identified in HSY$_{R2\text{-}IIIb}$ as tyrosine phosphorylated proteins.

Fig. 16. MAPK activities in HSYzeo.

MEK1/2 and p38 MAPK were phosphorylated in HSYzeo upon stimulation with either FGF-1 or FGF-2. Phosphorylated JNK was not observed in the cells.

Fig. 17. MAPK activities in HSY$_{R2\text{-}IIIb}$ stimulated with FGF-1 or FGF-2.

MEK1/2 was the only phosphorylated MAPK in HSY$_{R2\text{-}IIIb}$ by FGF-1, or FGF-2 stimulation.

Fig. 18. MAPK activities in HSY$_{R2\text{-}IIIb}$ stimulated with KGF.

Phosphorylation of MEK1/2 were detected in HSY$_{R2\text{-}IIIb}$ stimulated with KGF.

Fig. 19. MAPK activities in SGE.

Phosphorylation of MEK1/2 were detected in SGE stimulated with FGF-1 or KGF.

Fig.20. Immunohistochemical analysis for nuclear translocation of p38 MAPK in HSYzeo.

The expression and distribution of p38 MAPK in HSYzeo upon stimulation with FGFs were assessed by immunoperoxidase staining with anti-p38 and anti-phosphorylated-p38 antibodies. In G0-arrested HSYzeo, positive staining for p38 MAPK was observed in the cytoplasm (Fig.20**A**), but immuno-negative for phospho-p38 MAPK (Fig.20**B**). At 5 min after stimulation with FGF-1 or FGF-2, both p38 and phosphorylated-p38 were predominantly localized in the nucleus (Fig. 20**C** and 20**D**). At 2h after stimulation with FGF-1 or FGF-2, phosphorylated-p38 was uniformly localized in the whole cells (Fig.20**E**). The addition of p38 MAPK inhibitor SB203580 (5mM) prior to FGF-1 or FGF-2 treatment inhibited nuclear translocation of p38 MAPK in HSYzeo (Fig.20**F**). Scale bar: 20μm

Fig.21. Effects of MEK1/2 inhibitor and p38 inhibitor on the phosphorylation of p38 MAPK in HSYzeo by western blotting analysis.

1, control, **2**, FGF stimulation, **3**, FGF stimulation + MEK1/2 inhibitor, **4**, FGF stimulation + p38 inhibitor.

Fig. 22. Schematic presentation of electric pulse generator and EP condition.

Ex vivo EP of KGFR/FGFR2-IIIb gene into HSY-derived adenocarcinomas of living athymic mouse was carried out. Pulses were given to the tumors by a pair of needle-type electrode, which were inserted subcutaneously around the tumors. 8 pulses were administrated at a rate of one pulse per second. Electric pulses were 50 m sec in duration at 50 or 70 voltage.

Fig. 23. Macroscopic appearance and growth of HSY-derived tumors treated with KGFR gene therapy at 1 week after tumor inoculation.

At 1 week after HSY cell inoculation, pcDNA3.1/zeo-KGFR/FGFR2-IIIb or empty vector was electro-transferred into tumors. The size of tumors became smaller within 1 week after EP (KGFR) and then disappeared. The tumors electro-transferred with empty pcDNA3.1/zeo vector (control) showed high growth rate.

Fig. 24. Macroscopic appearance and growth of HSY-derived tumors treated with KGFR gene therapy at 4 week after tumor inoculation.

At 4 weeks after HSY cell inoculation, pcDNA3.1/zeo-KGFR/FGFR2-IIIb or empty vector was electro-transferred into tumors. The growth rate of tumors was inhibited significantly, but none of tumor were disappeared (KGFR). The tumors electro-transferred with empty pcDNA3.1/zeo vector (control) showed high growth rate.

Fig. 25. Expression of KGFR in HSY tumors treated with KGFR gene therapy.

Efficacy of KGFR/FGFR2-IIIb gene transfer by EP was evaluated by immunohistochemical study using anti-FGFR2-IIIb (anti-bek) antibody. At 48 hours after gene transfer, about 70% of tumor cells exhibited KGFR/FGFR2-IIIb expression in the nucleus and cytoplasm (**A**). KGFR/FGFR2-IIIb was still expressed in 1 (**B**) and 4 weeks (**C**) after EP. There were no expression of KGFR/FGFR2-IIIb in the tumors transferred with empty vector (**D**). Magnification: x100.

Fig. 26. Immunoperoxidase staining for KGFR and TUNEL staining for apoptosis in HSY-derived tumors treated with KGFR gene therapy.

Immunoperoxidase staining for KGFR (**A**) (magnification: x400), HE staining (**B**) (magnification: x400) and TUNEL stainig (**Inset**) of HSY-derived tumors treated with KGFR gene therapy. Tumor cells expressing KGFR also exhibited TUNEL positive staining.

Table 1. KGFR numbers and dissociation constant (kd) in HSY$_{R2\text{-}IIIb}$.

7 clones exhibiting high binding capacity to KGF were isolated and designated HSY$_{R2\text{-}IIIb}$ (clone 2-4-2, 6-4-3, 6-3-9, 6-1-9, 6-4-5, 24-3-9, 24-2-2). Scatchard plots analysis revealed that the presence of a sigle high-affinity receptor population of 0.79-5.66x10^5 sites per cell with an apparent dissociation constant (kd) of 1.48-10.6x10^{-11}M.

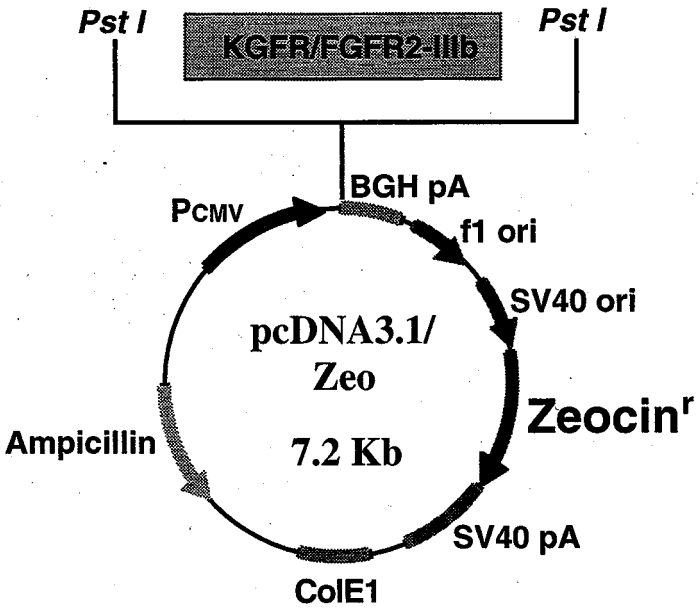

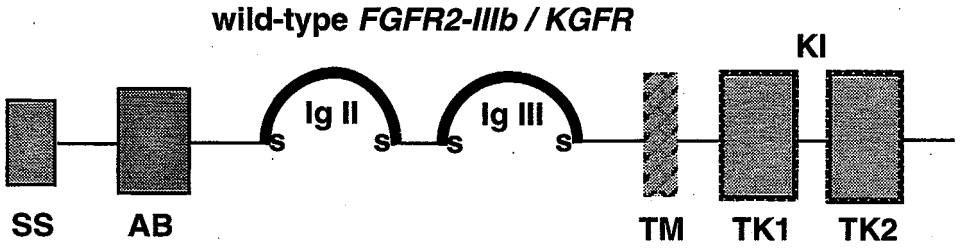

SS: Signal Sequence
AB: Acidic Box
TM: Transmembrane
KI: Kinase Insertion
TK: Tyrosine Kinase

Fig. 1

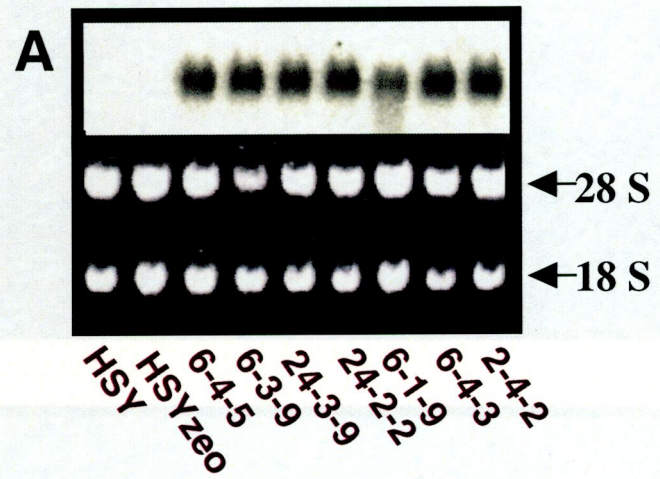
A
28 S
18 S
HSY
HSYzeo
6-4-5
6-3-9
24-3-9
24-2-2
6-1-9
6-4-3
2-4-2

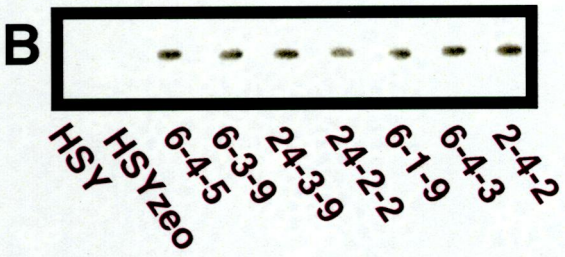
B
HSY
HSYzeo
6-4-5
6-3-9
24-3-9
24-2-2
6-1-9
6-4-3
2-4-2

Fig. 2

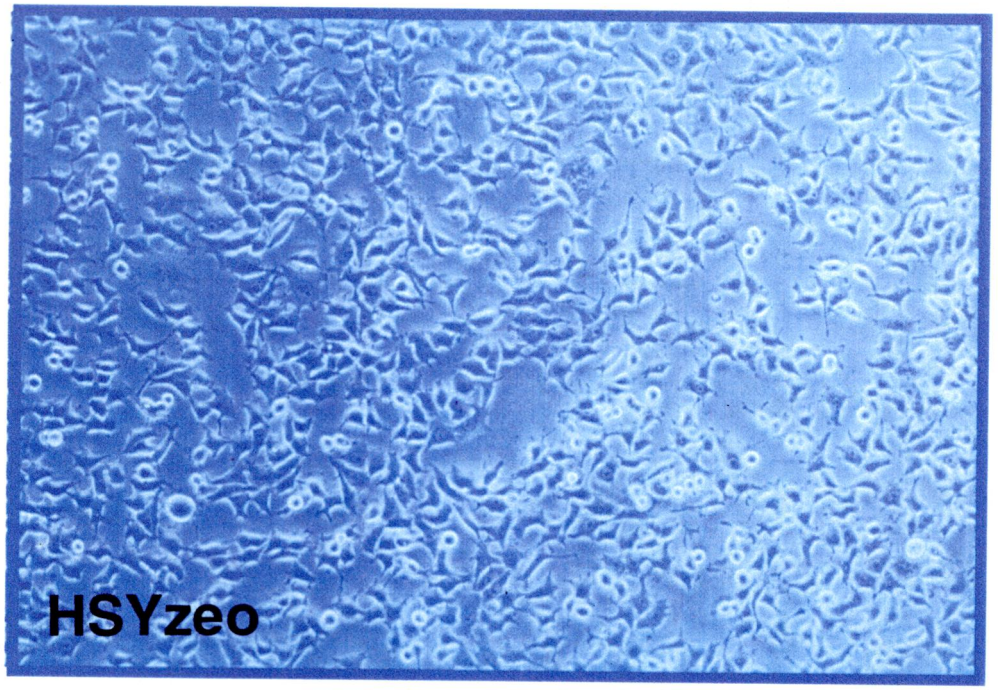

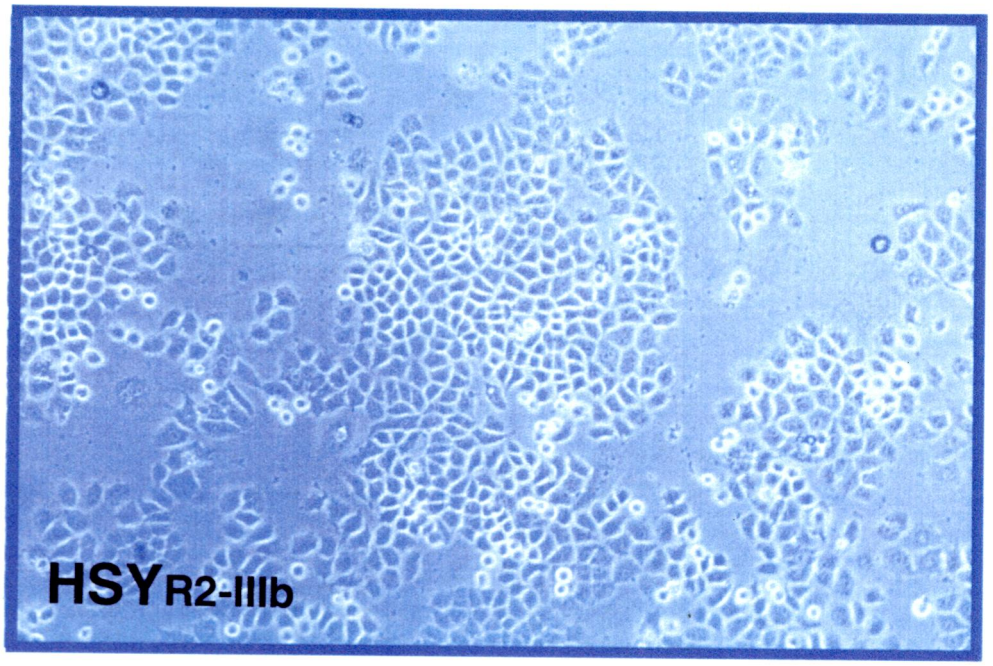

Fig. 3

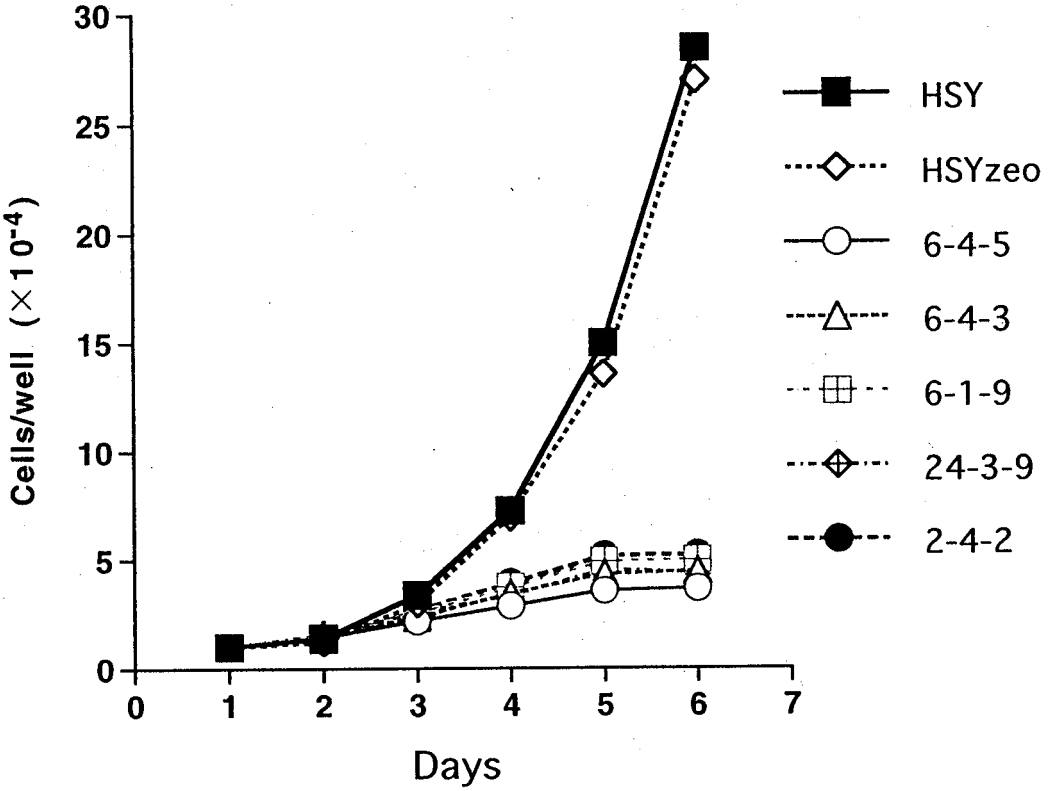
30
25
20
15
10
5
0
Cells/well (×10⁻⁴)
0
1
2
3
4
5
6
7
Days
HSY
HSYzeo
6-4-5
6-4-3
6-1-9
24-3-9
2-4-2

Fig. 4

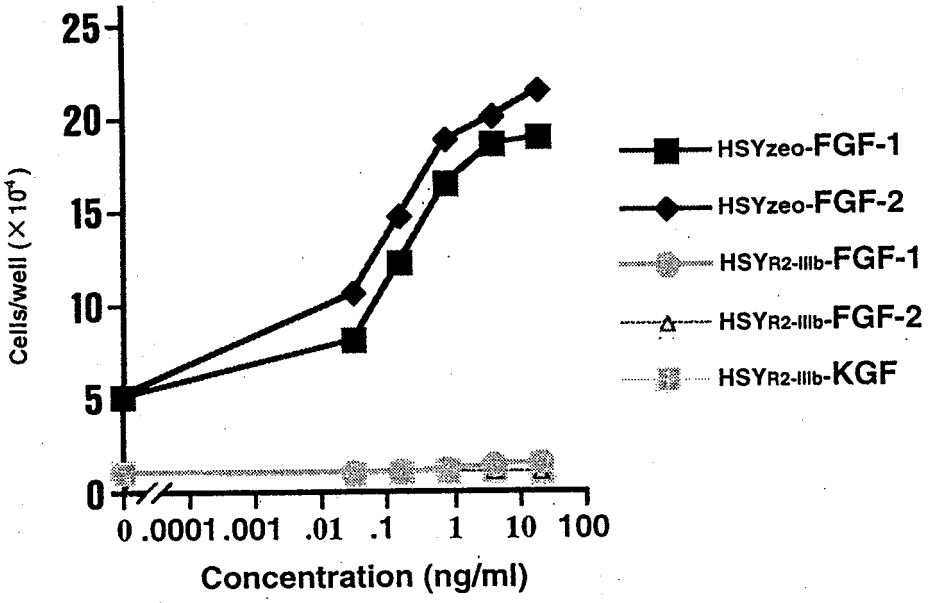
25
20
15
10
5
0
Cells/well (×10⁴)
0 .0001 .001 .01 .1 1 10 100
Concentration (ng/ml)
HSYzeo-FGF-1
HSYzeo-FGF-2
HSYR2-IIIb-FGF-1
HSYR2-IIIb-FGF-2
HSYR2-IIIb-KGF

Fig. 5

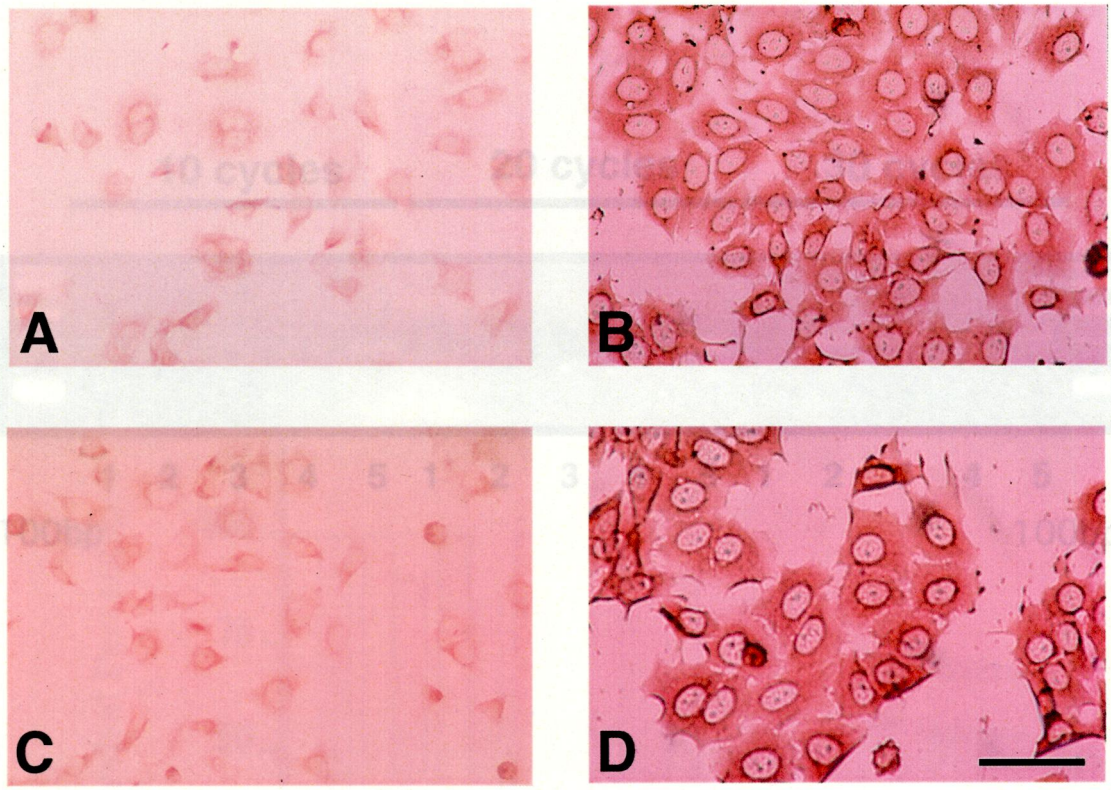

Fig. 6

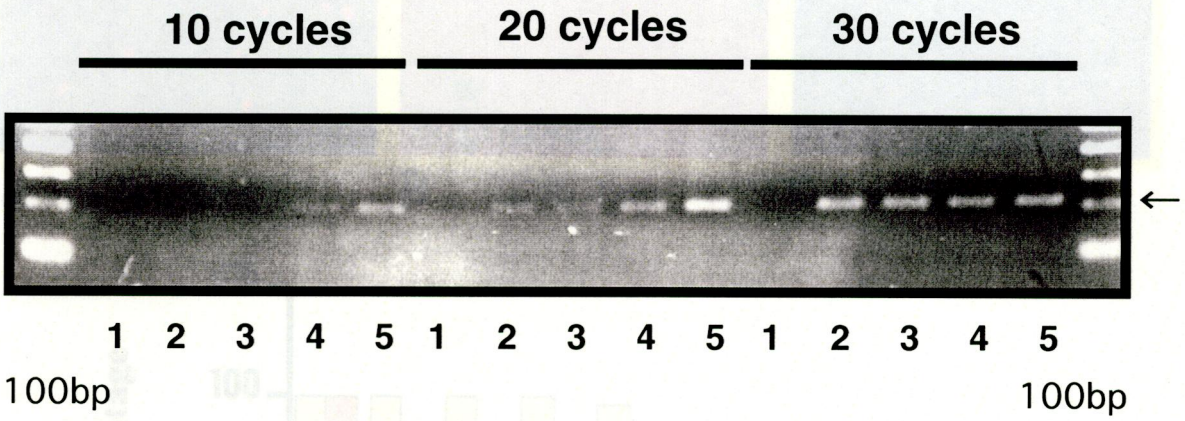

Fig. 7

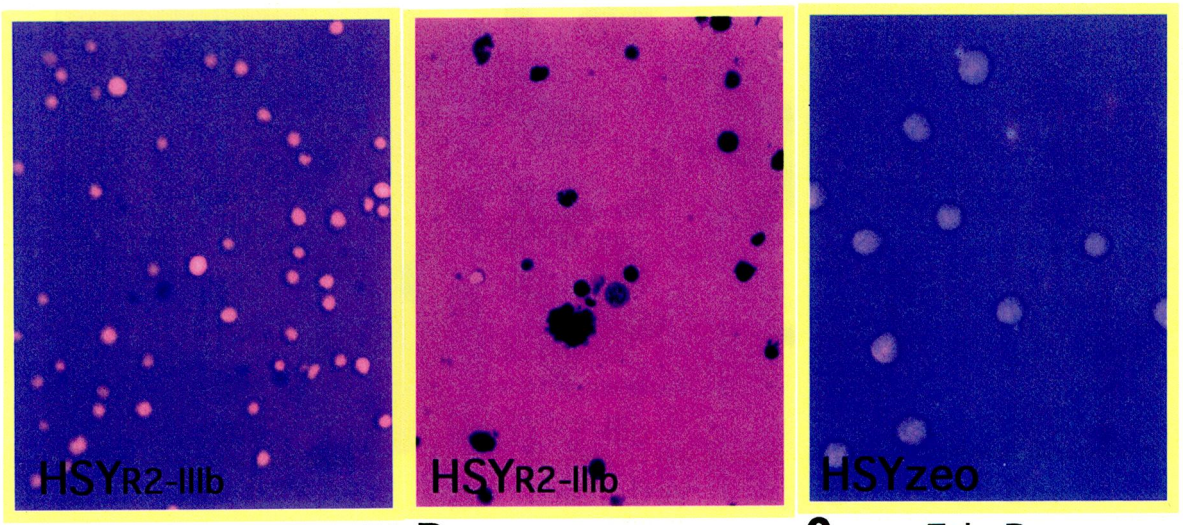

A 1st. Day B 7th. Day C 7th. Day

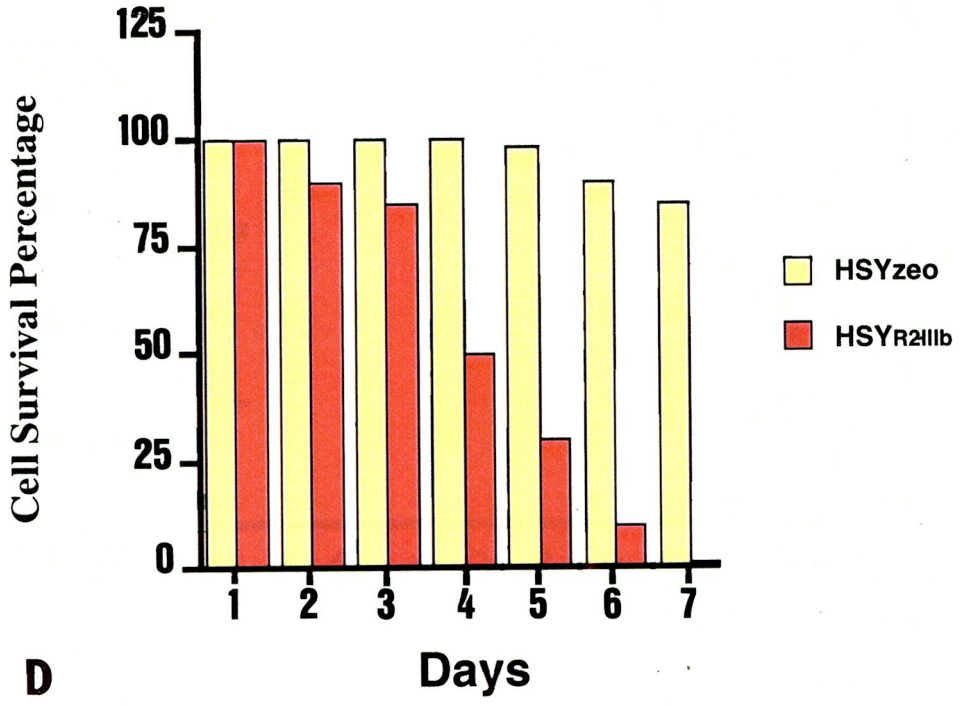

D

Fig. 8

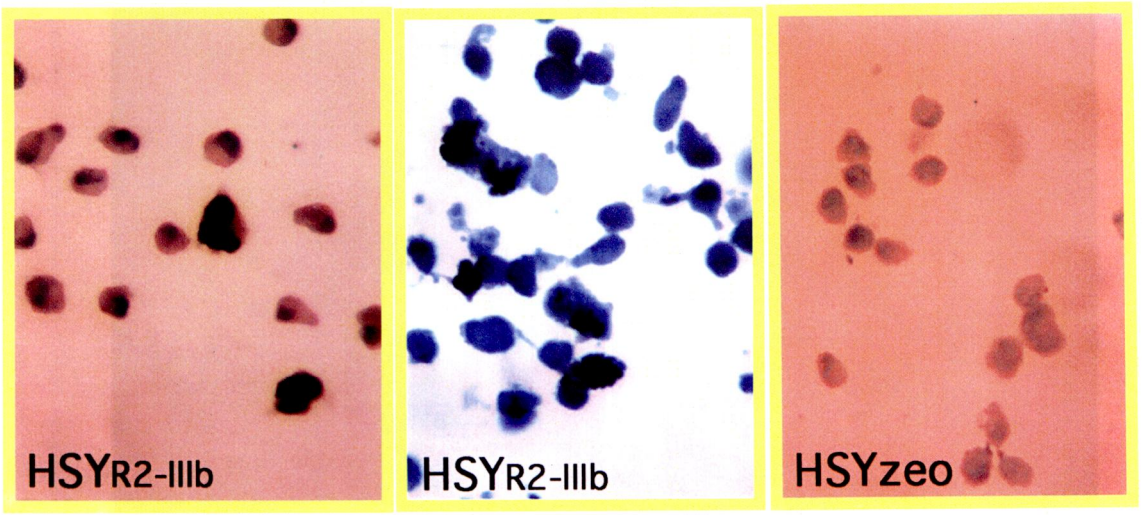

A 1st. Day **B** 7th. Day **C** 7th. Day

D

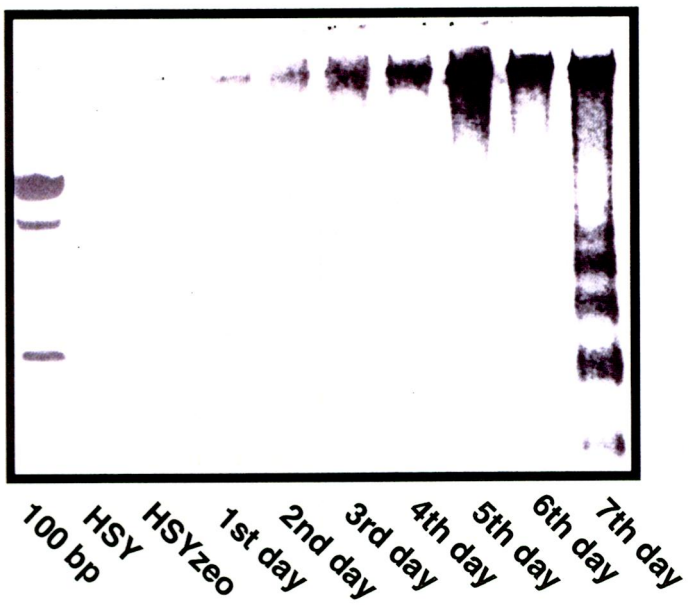

Fig. 9

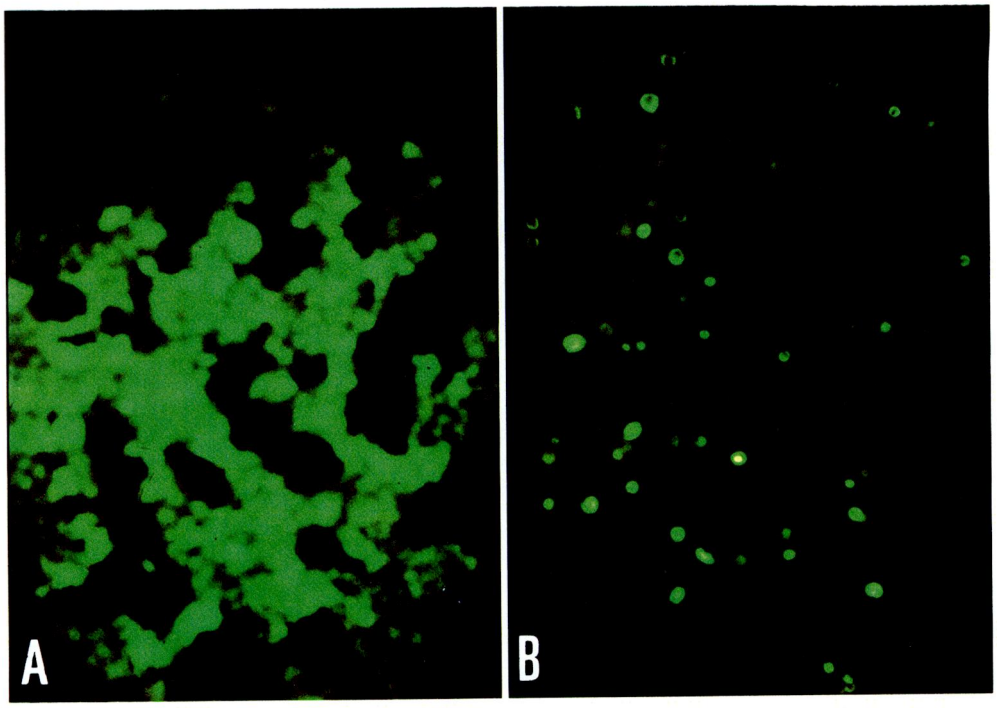
A
B

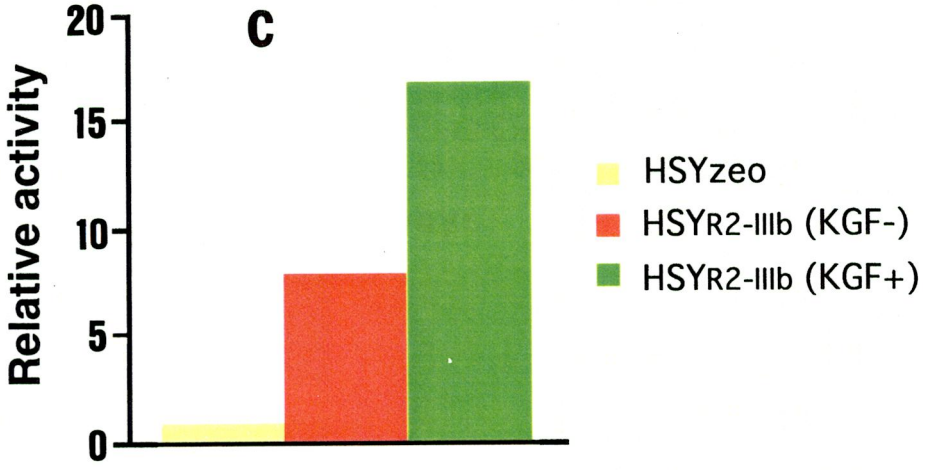
C
Relative activity
20
15
10
5
0
HSYzeo
HSYR2-IIIb (KGF-)
HSYR2-IIIb (KGF+)

Fig. 10

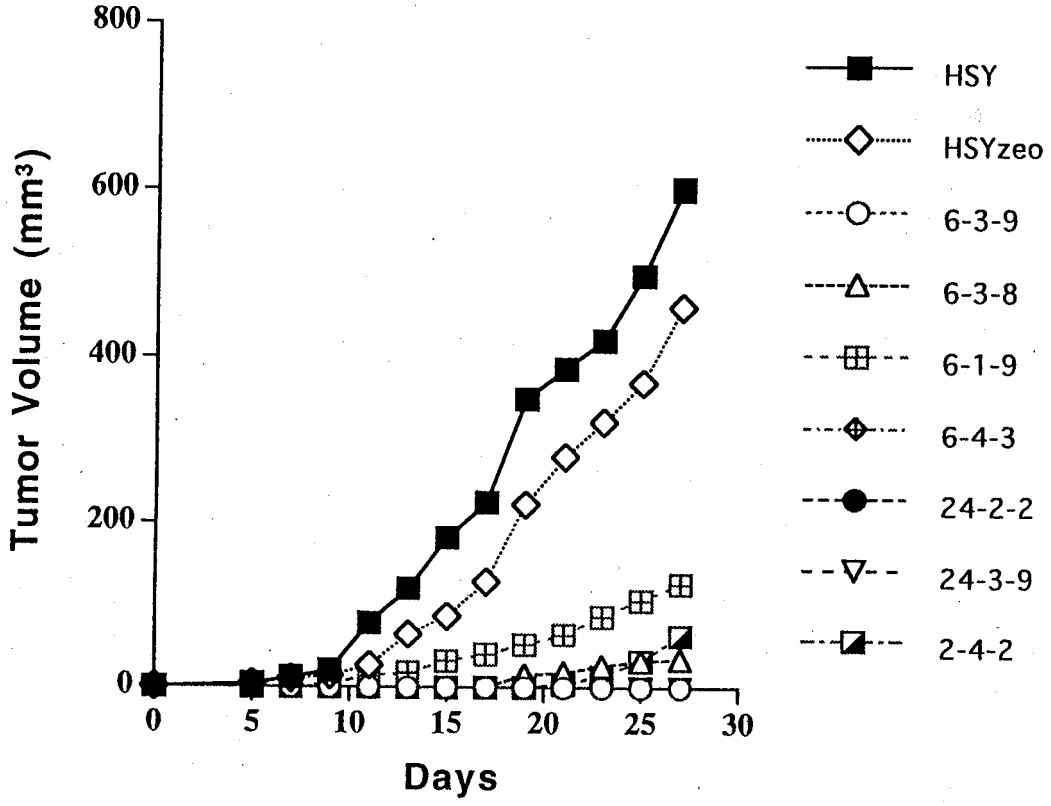
800
600
400
200
0
Tumor Volume (mm³)
0
5
10
15
20
25
30
Days
HSY
HSYzeo
6-3-9
6-3-8
6-1-9
6-4-3
24-2-2
24-3-9
2-4-2

Fig. 11

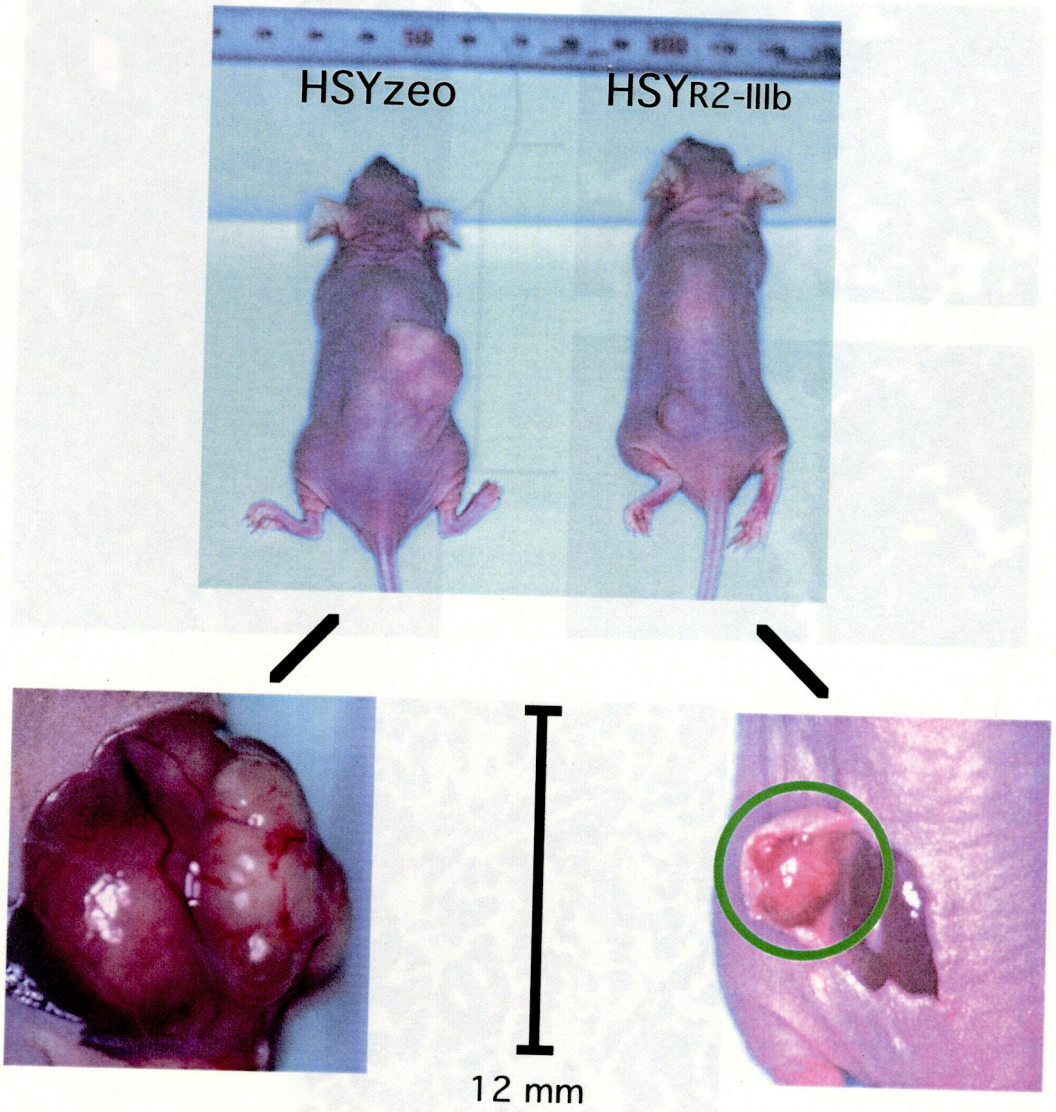

Fig. 12

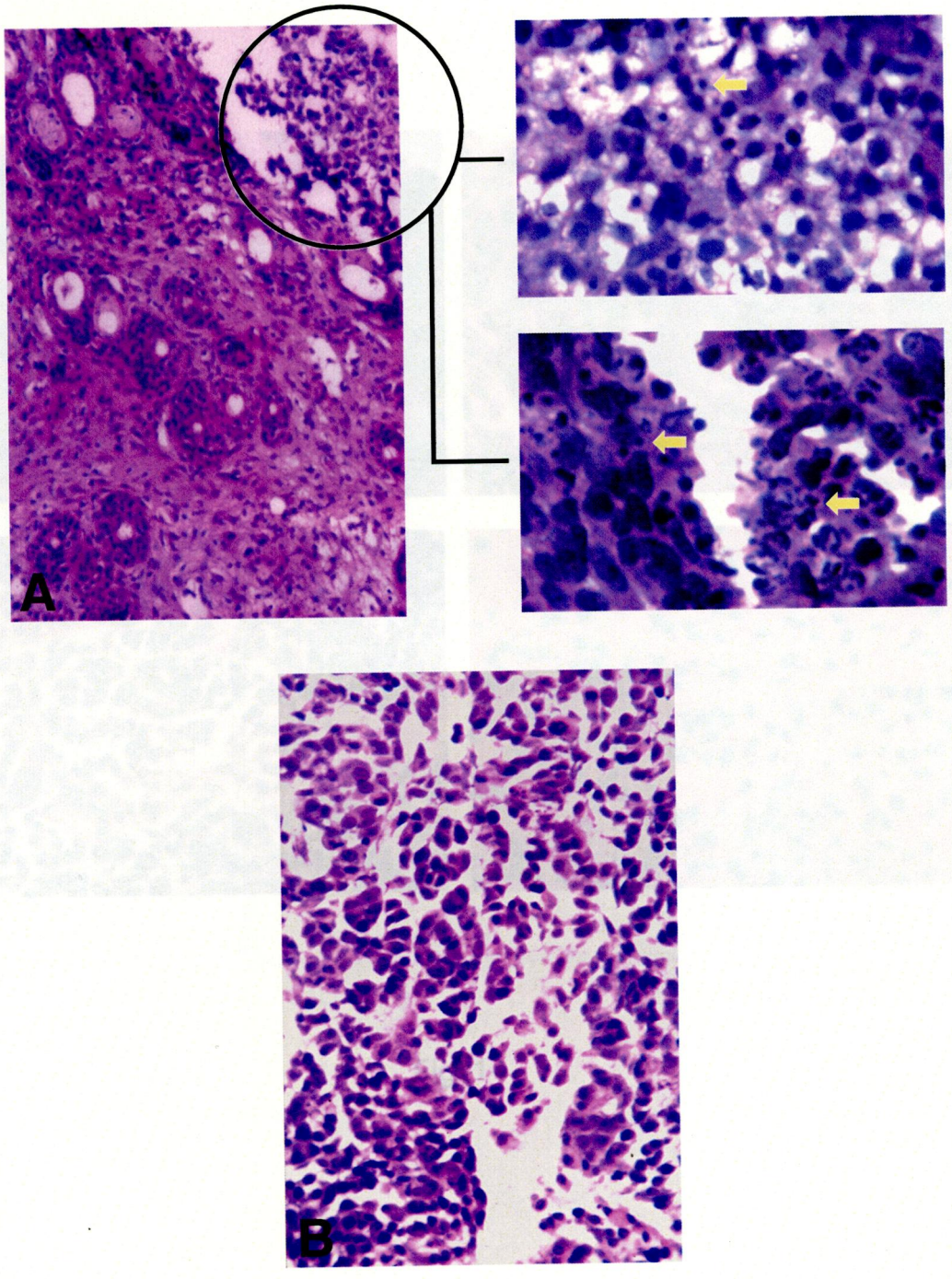

Fig. 13

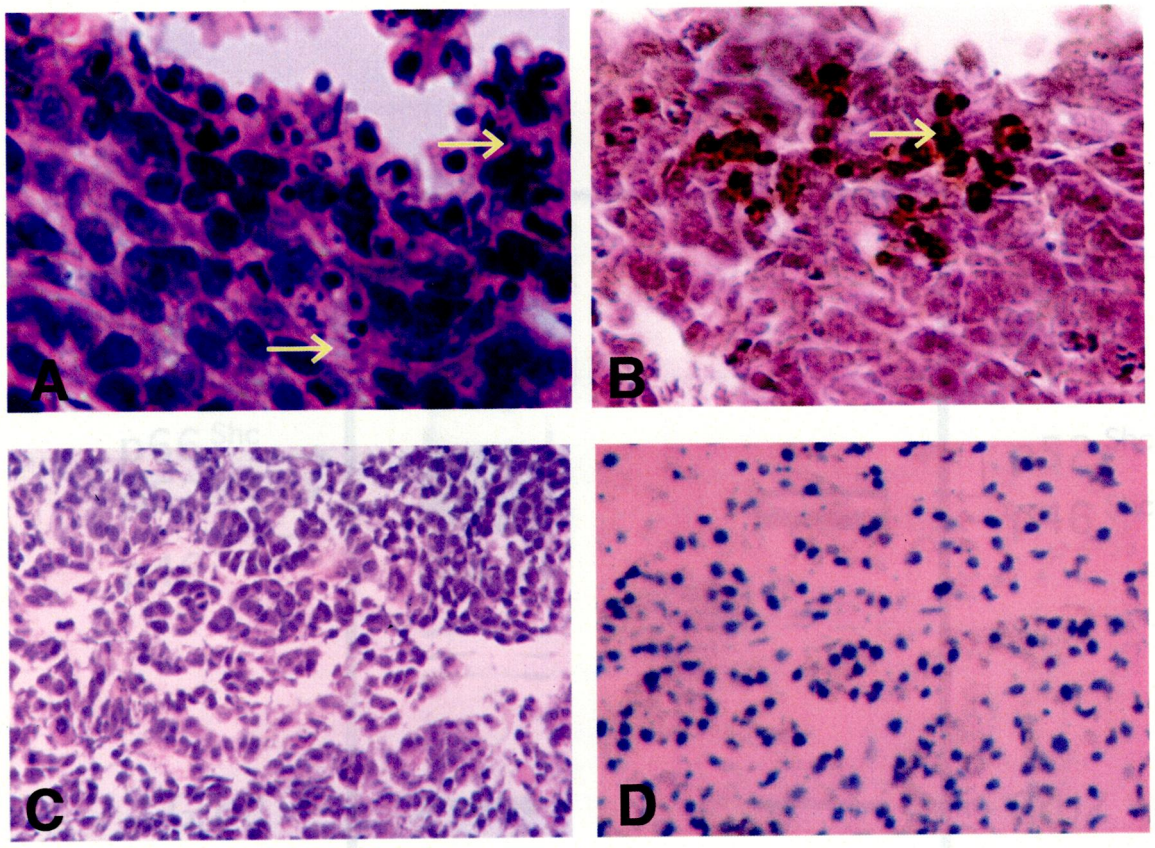

Fig. 14

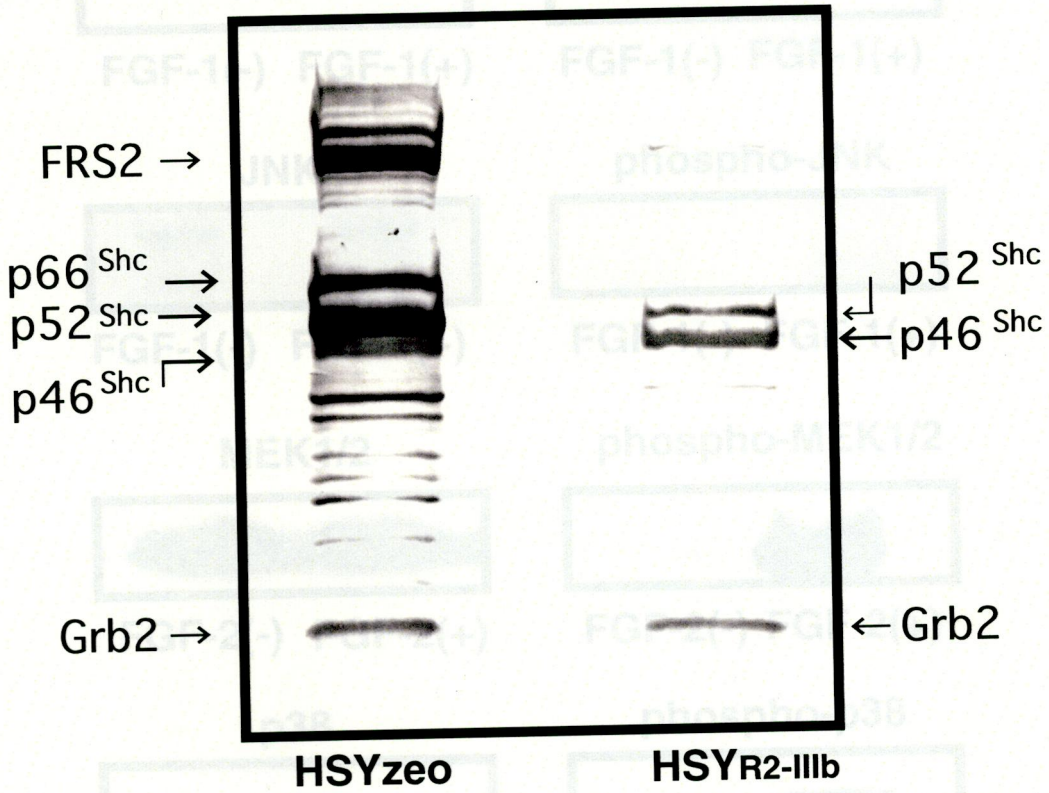
FRS2 →
p66 Shc →
p52 Shc →
p46 Shc →
Grb2 →
p52 Shc
← p46 Shc
← Grb2
HSYzeo
HSYR2-IIIb

Fig. 15

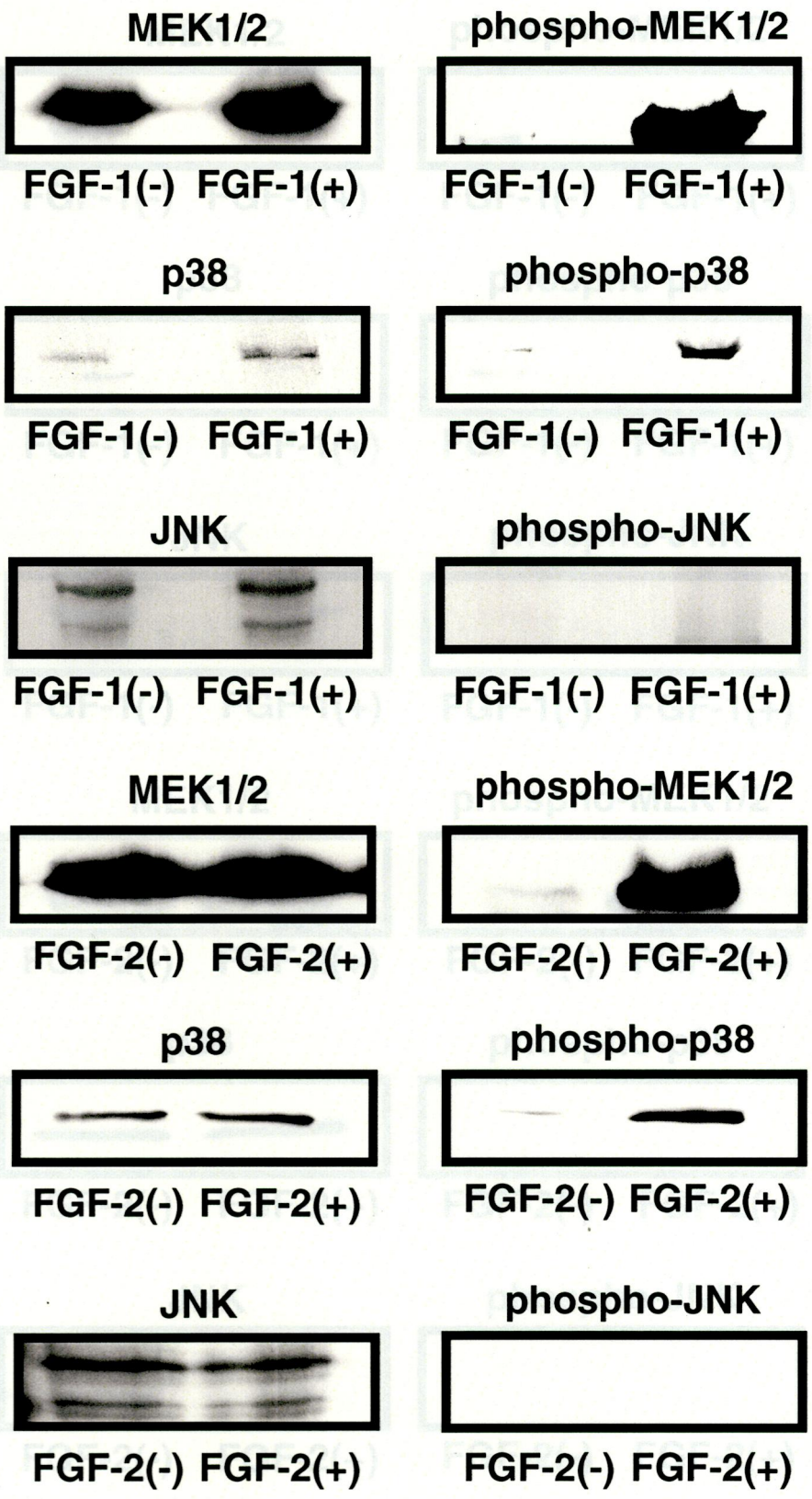
MEK1/2
phospho-MEK1/2
FGF-1(-) FGF-1(+)
FGF-1(-) FGF-1(+)
p38
phospho-p38
FGF-1(-) FGF-1(+)
FGF-1(-) FGF-1(+)
JNK
phospho-JNK
FGF-1(-) FGF-1(+)
FGF-1(-) FGF-1(+)
MEK1/2
phospho-MEK1/2
FGF-2(-) FGF-2(+)
FGF-2(-) FGF-2(+)
p38
phospho-p38
FGF-2(-) FGF-2(+)
FGF-2(-) FGF-2(+)
JNK
phospho-JNK
FGF-2(-) FGF-2(+)
FGF-2(-) FGF-2(+)

Fig. 16

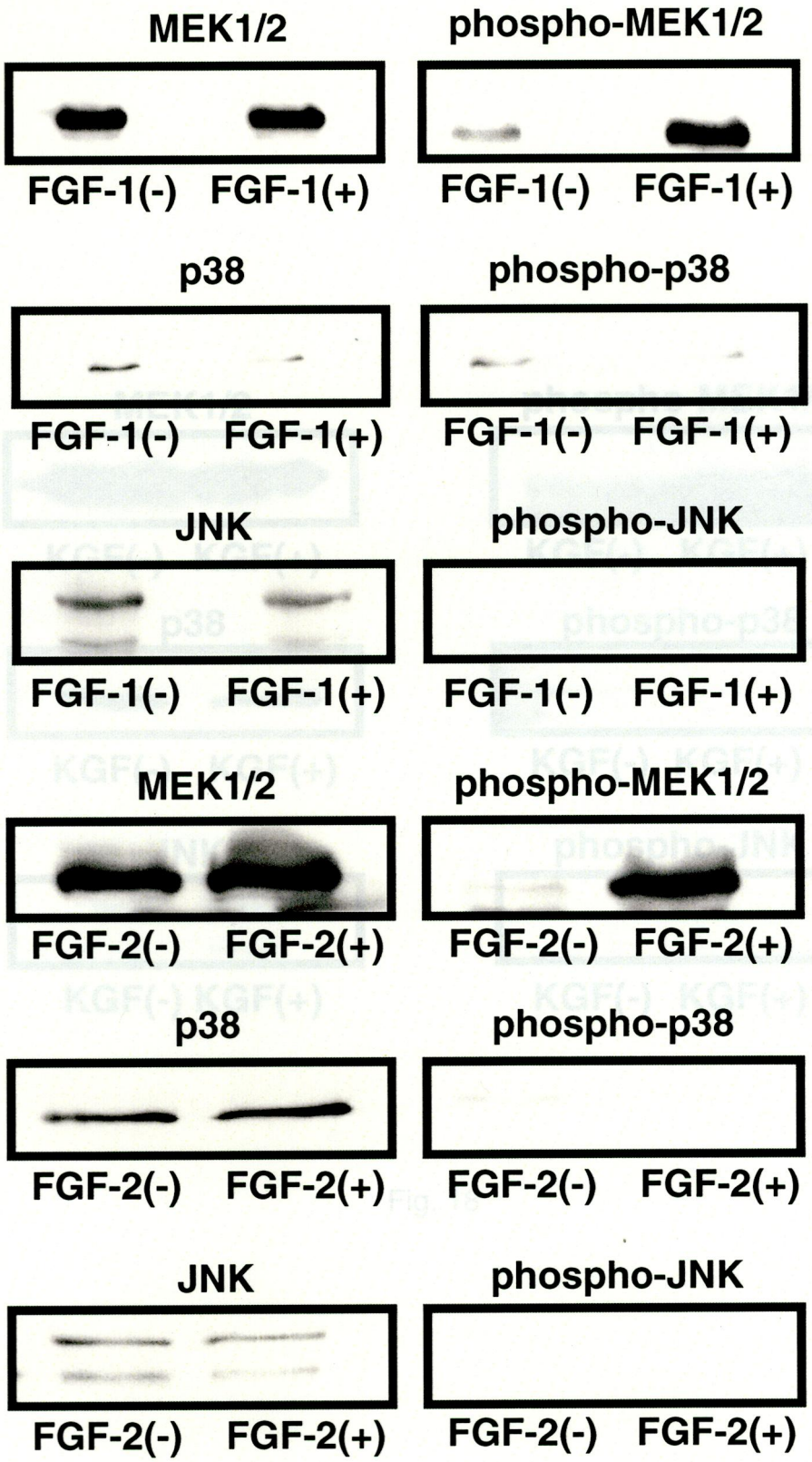
MEK1/2
phospho-MEK1/2
FGF-1(-) FGF-1(+)
FGF-1(-) FGF-1(+)
p38
phospho-p38
FGF-1(-) FGF-1(+)
FGF-1(-) FGF-1(+)
JNK
phospho-JNK
FGF-1(-) FGF-1(+)
FGF-1(-) FGF-1(+)
MEK1/2
phospho-MEK1/2
FGF-2(-) FGF-2(+)
FGF-2(-) FGF-2(+)
p38
phospho-p38
FGF-2(-) FGF-2(+)
FGF-2(-) FGF-2(+)
JNK
phospho-JNK
FGF-2(-) FGF-2(+)
FGF-2(-) FGF-2(+)

Fig. 17

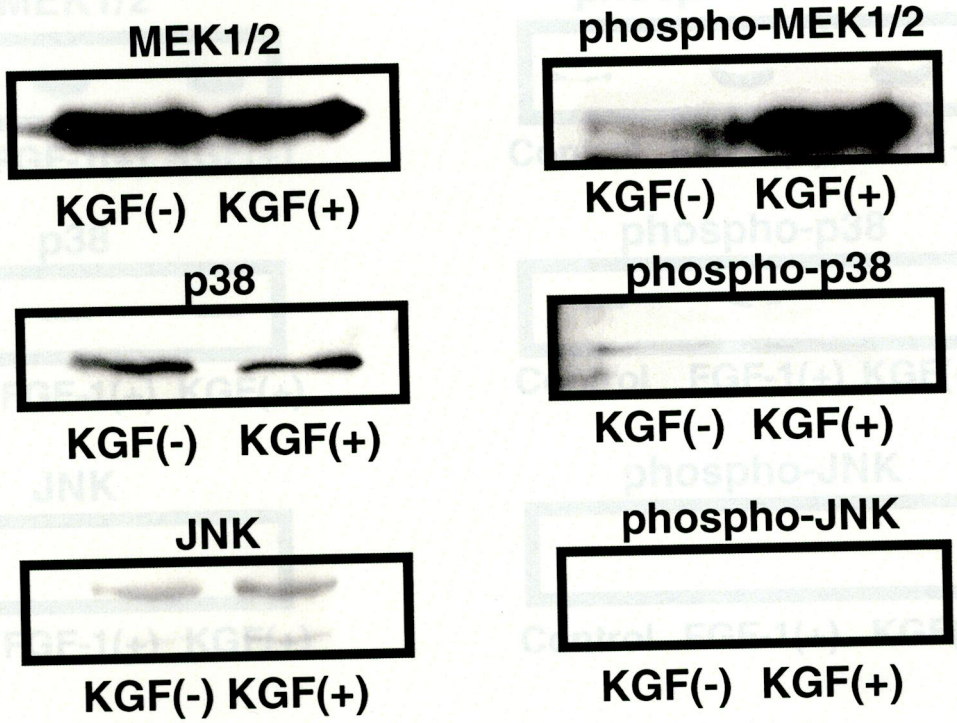
MEK1/2
KGF(-) KGF(+)
phospho-MEK1/2
KGF(-) KGF(+)
p38
KGF(-) KGF(+)
phospho-p38
KGF(-) KGF(+)
JNK
KGF(-) KGF(+)
phospho-JNK
KGF(-) KGF(+)

Fig. 18

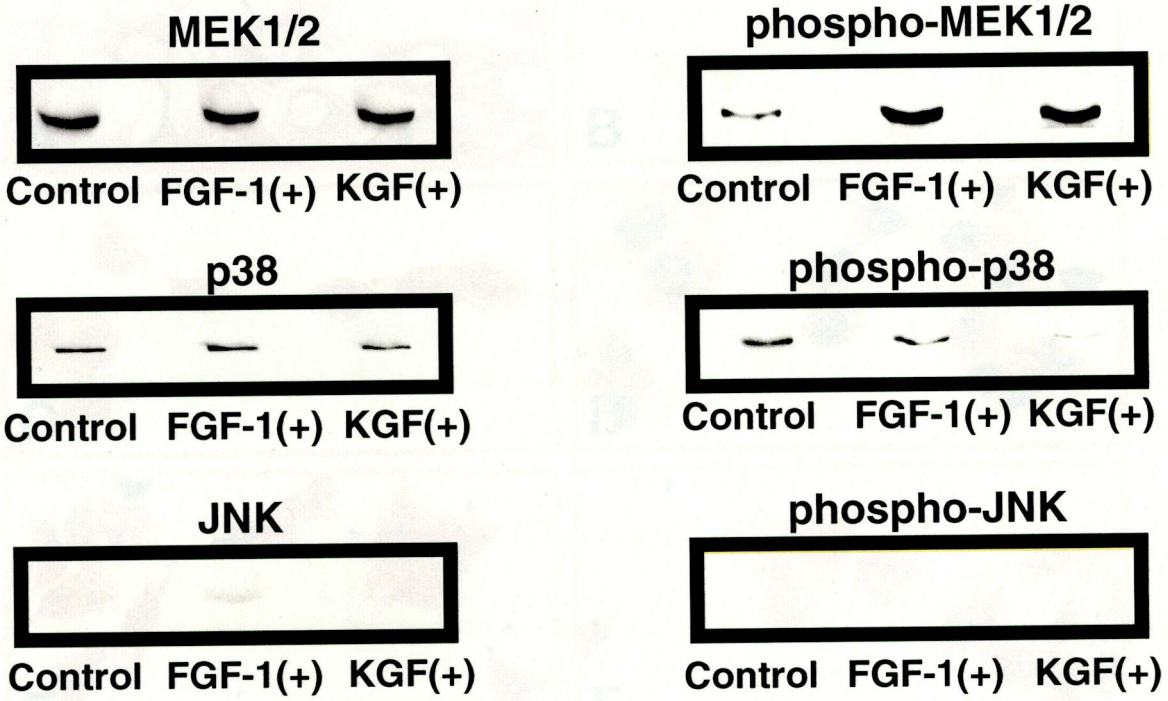
MEK1/2
Control FGF-1(+) KGF(+)
phospho-MEK1/2
Control FGF-1(+) KGF(+)
p38
Control FGF-1(+) KGF(+)
phospho-p38
Control FGF-1(+) KGF(+)
JNK
Control FGF-1(+) KGF(+)
phospho-JNK
Control FGF-1(+) KGF(+)

Fig. 19

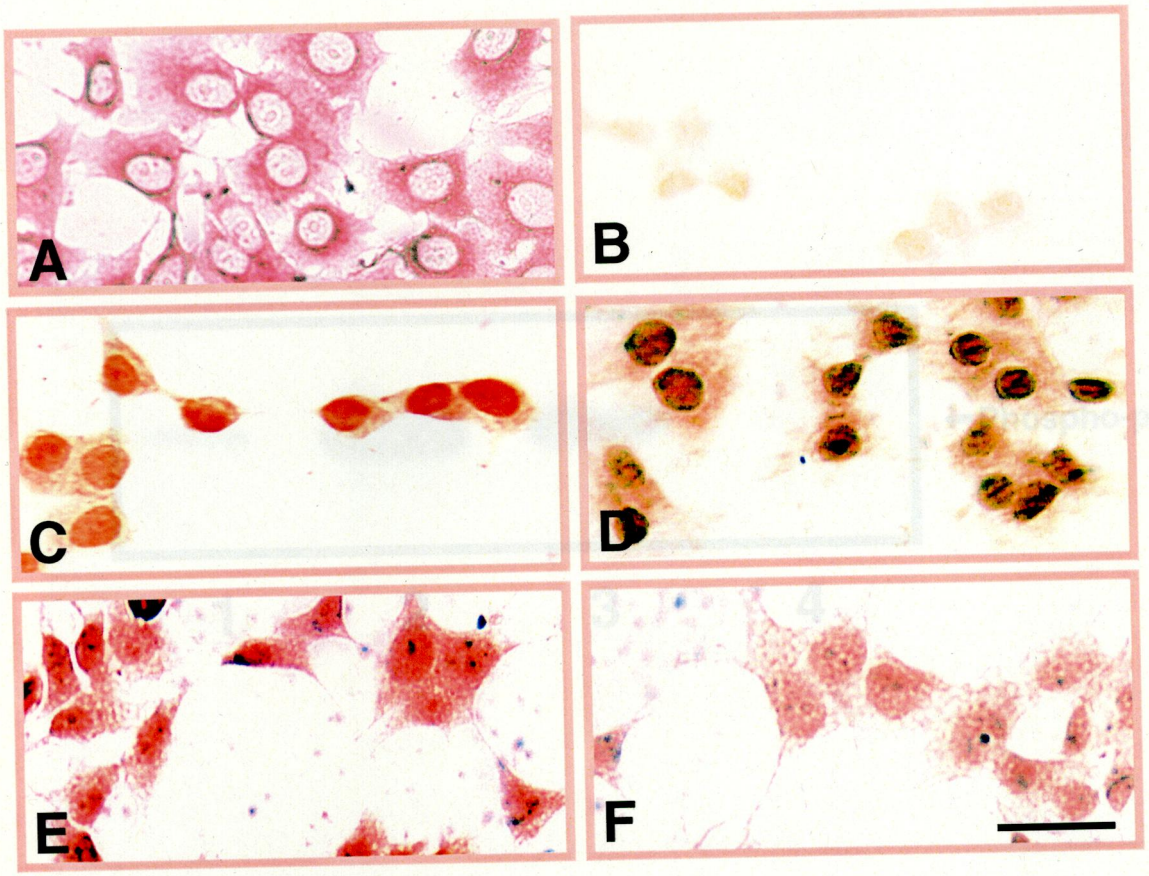

Fig. 20

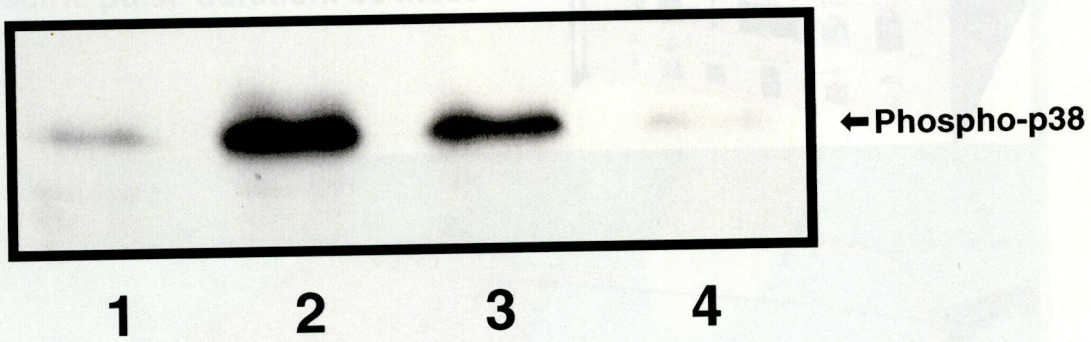

Fig. 21

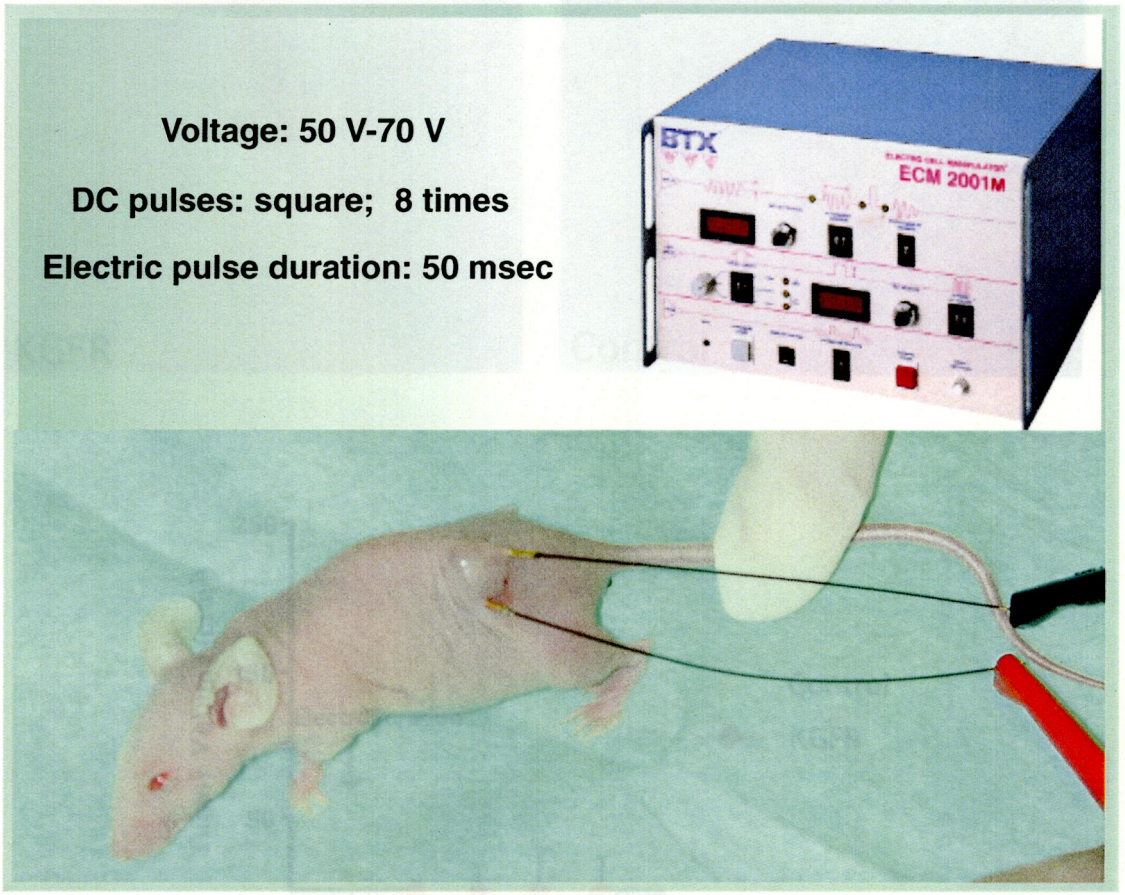
Voltage: 50 V-70 V
DC pulses: square; 8 times
Electric pulse duration: 50 msec
BTX
ECM 2001M

Fig. 22

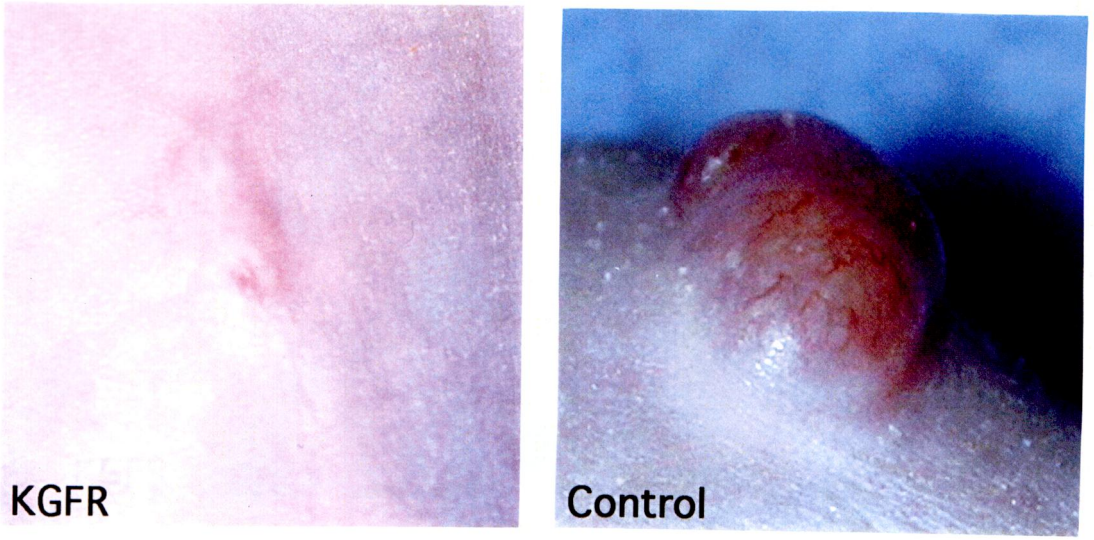
KGFR
Control

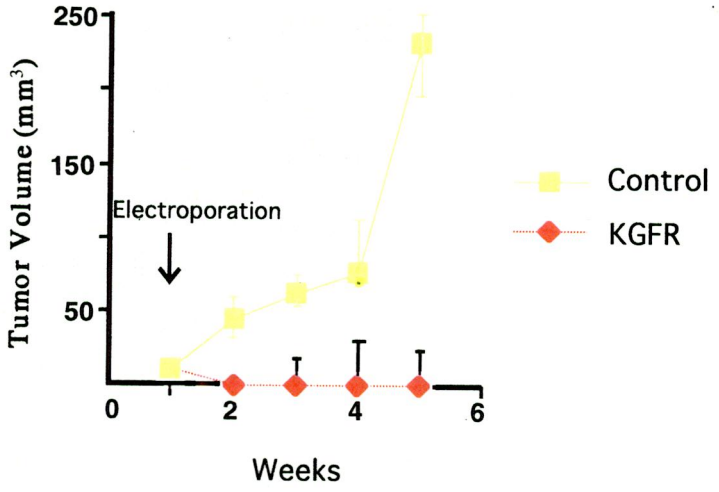
250
150
50
Tumor Volume (mm3)
Electroporation
0
2
4
6
Weeks
Control
KGFR

Fig. 23

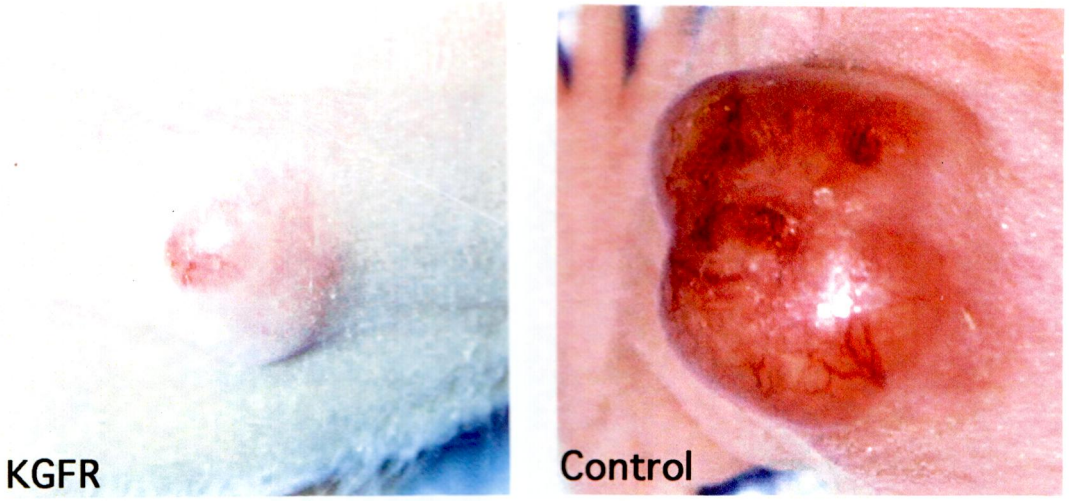
KGFR
Control

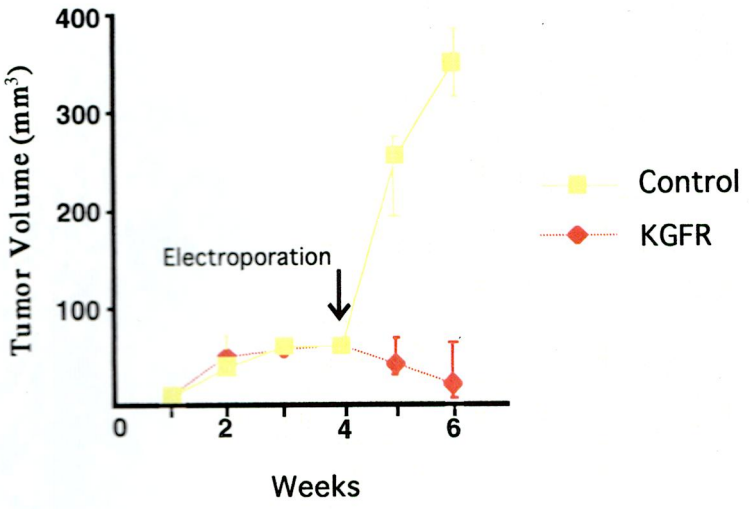
400
300
200
100
Tumor Volume (mm3)
Electroporation
0
2
4
6
Weeks
Control
KGFR

Fig. 24

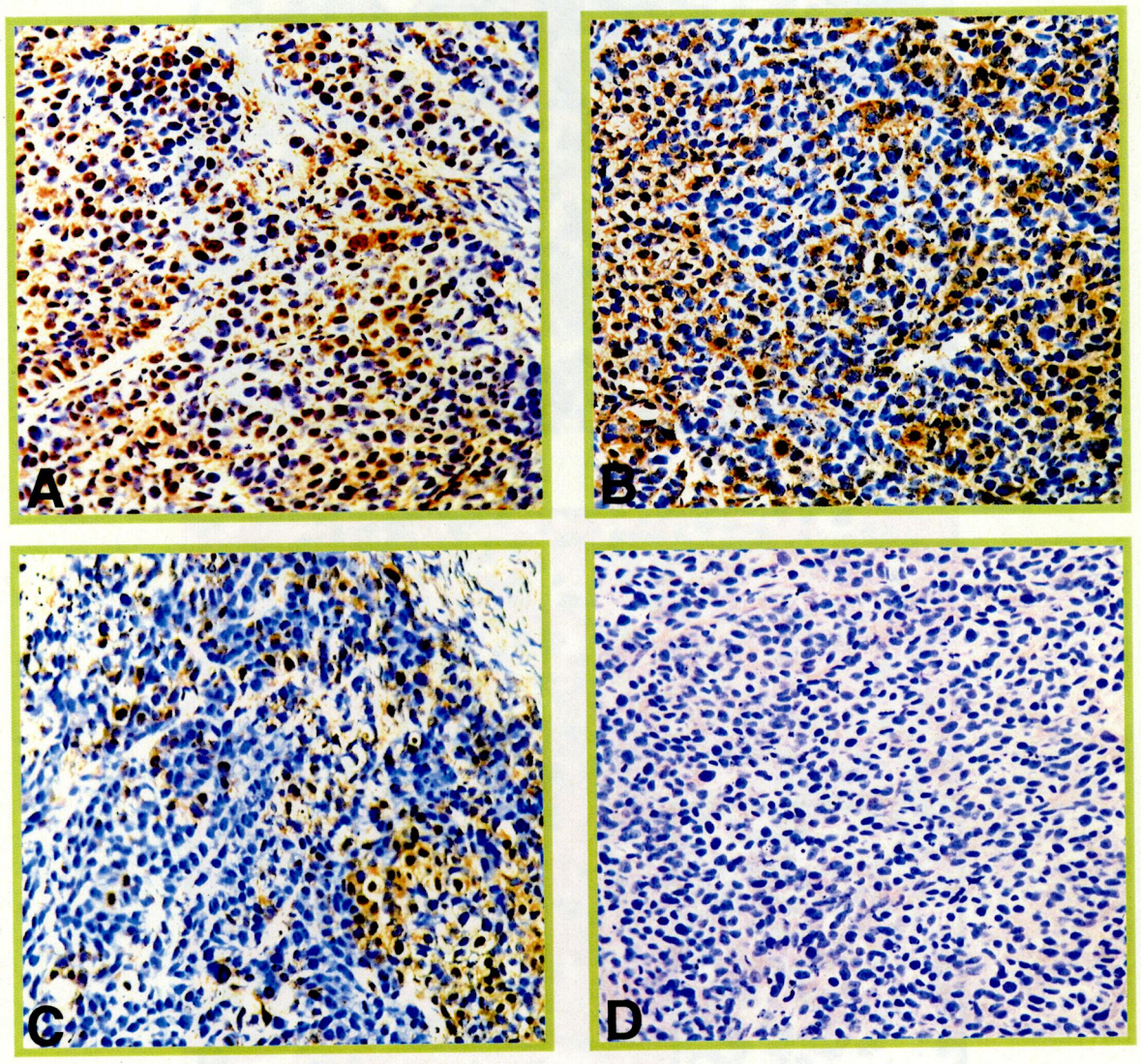

Fig. 25

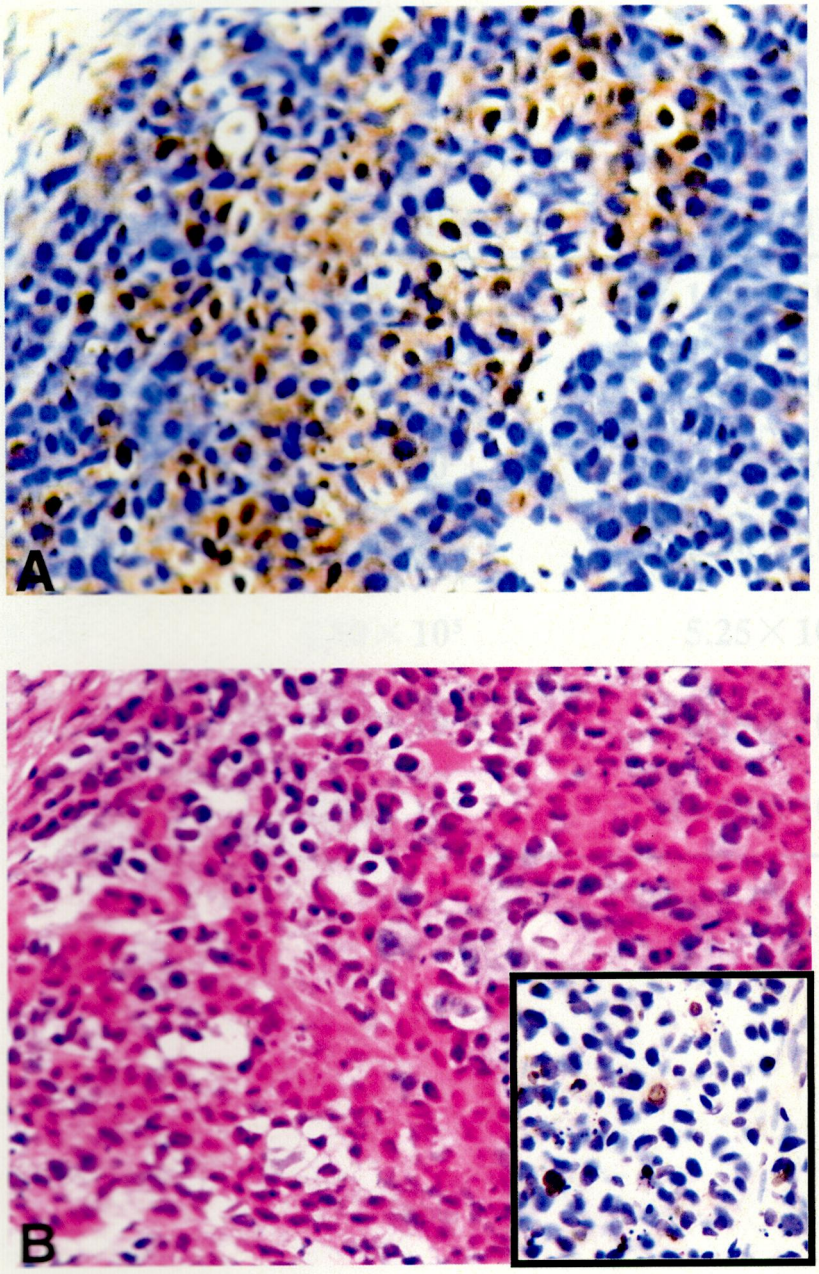

Fig. 26

Clone	Receptor Number/cell	*Kd* (M)
24-2-2	0.79×10^{5}	1.48×10^{-11}
6-3-9	1.20×10^{5}	2.25×10^{-11}
6-1-9	1.59×10^{5}	2.98×10^{-11}
6-4-5	1.76×10^{5}	3.30×10^{-11}
24-3-9	2.80×10^{5}	5.25×10^{-11}
2-4-2	3.30×10^{5}	6.19×10^{-11}
6-4-3	5.66×10^{5}	10.60×10^{-11}

Table 1